Geoscience Frontiers 11 (2020) 719–738

HOSTED BY

Contents lists available at ScienceDirect

Geoscience Frontiers

journal homepage: www.elsevier.com/locate/gsf

Focus Paper

A scale-integrated exploration model for orogenic gold deposits based on a mineral system approach

David I. Groves [a,b], M. Santosh [b,c,d,*], Liang Zhang [b]

[a] Orebusters Pty Ltd, Gwelup, 6018, WA, Australia
[b] State Key Laboratory of Geological Processes and Mineral Resources, China University of Geosciences (Beijing), Beijing, 100083, China
[c] Dept. of Earth Sciences, University of Adelaide, SA, 5005, Australia
[d] Yonsei Frontier Lab, Yonsei University, Seoul, 120-749, Republic of Korea

ARTICLE INFO

Handling Editor: Vinod Oommen Samuel

Keywords:
Mineral systems
Orogenic gold
Sub-crustal fluids
Convergent margins
Gold exploration

ABSTRACT

Concept-based orogenic gold exploration requires a scale-integrated approach using a robust mineral system model. Most genetic hypotheses for orogenic gold deposits that involve near-surface or magmatic-hydrothermal fluids are now negated in terms of a global mineral system model. Plausible models involve metamorphic fluids, but the fluid source has been equivocal. Crustal metamorphic-fluid models are most widely-accepted but there are serious problems for Archean deposits, and numerous Chinese provinces, including Jiaodong, where the only feasible fluid source is sub-crustal. If all orogenic gold deposits define a coherent mineral system, there are only two realistic sources of fluid and gold, based on their syn-mineralization geodynamic settings. These are from devolatilization of a subducted oceanic slab with its overlying gold-bearing sulfide-rich sedimentary package, or release from mantle lithosphere that was metasomatized and fertilized during a subduction event, particularly adjacent to craton margins. In this model, CO_2 is generated during decarbonation and S and ore-related elements released from transformation of pyrite to pyrrhotite at about 500 °C. This orogenic gold mineral system can be applied to conceptual exploration by first identifying the required settings at geodynamic to deposit scales. Within these settings, it is then possible to define the critical gold mineralization processes in the system: fertility, architecture, and preservation. The geological parameters that define these processes, and the geological, geophysical and geochemical proxies and responses for these critical parameters can then be identified. At the geodynamic to province scales, critical processes include a tectonic thermal engine and deep, effective, fluid plumbing system driven by seismic swarms up lithosphere-scale faults in an oblique-slip regime during uplift late in the orogenic cycle of a convergent margin. At the district to deposit scale, the important processes are fluid focussing into regions of complex structural geometry adjacent to crustal-scale plumbing systems, with gold deposition in trap sites involving complex conjugations of competent and/or reactive rock sequences and structural or lithological fluid caps. Critical indirect responses to defined parameters change from those generated by geophysics to those generated by geochemistry with reduction in scale of the mineral system-driven conceptual exploration.

1. Introduction

There are broadly two types of mineral exploration, commonly termed brownfield and greenfield exploration. Brownfield exploration involves exploration within, or in close proximity to, existing mineral deposits. Such exploration has the potential to provide continued production into the immediate to foreseeable future. For example, a very good case is mounted by Vearncombe and Phillips (2019) for the gold deposits of the Yilgarn Block of Western Australia. However, in the longer term, greenfield exploration is required to replenish depleted resources and maintain long-term production. This may be carried out distant from already-discovered deposits in known well-endowed mineral provinces (McCuaig et al., 2010), or in new exploration spaces with limited pre-competitive data (Joly et al., 2010). Unfortunately, mineral exploration, particularly in greenfields, is currently an inefficient process with discovery rates, particularly for gold, slowing significantly in the 21st Century (Schodde, 2017). This is despite increased exploration expenditure, as explorers are increasingly required to explore under regolith cover in available exploration spaces.

As Hronsky and Groves (2008) discuss, conceptual geological

* Corresponding author. State Key Laboratory of Geological Processes and Mineral Resources, China University of Geosciences (Beijing), Beijing, 100083, China.
E-mail addresses: m.santosh@adelaide.edu.au, santosh@cugb.edu.cn (M. Santosh).
Peer-review under responsibility of China University of Geosciences (Beijing).

https://doi.org/10.1016/j.gsf.2019.12.007
Received 20 November 2019; Received in revised form 27 December 2019; Accepted 30 December 2019
Available online 2 January 2020

targeting is required as an initial step to focus exploration into the most prospective districts within potentially well-endowed terranes or provinces. As a crucial first step, this requires the establishment of superior predictive geological models for the deposit type that is sought by the greenfield exploration program. This paper seeks to establish such a holistic model, via a mineral systems approach, for orogenic gold deposits. This is followed by discussion of the geological, geophysical and geochemical proxies for the various parameters required to adapt the conceptual model into a pragmatic exploration targeting model. The paper does not discuss the various methodologies that attempt to provide a quantitative measure of the endowment of any particular orogenic gold province (see Davies et al., 2018, 2019 and references therein for a recent review of a specific belt). It rather discusses the proxies for critical conceptual parameters that should drive identification of prospective orogenic gold provinces and geoscientific exploration within them.

2. Mineral systems approach

Research into genetic models for mineralization systems has gradually evolved over time from purely deposit-based models to more holistic models that view the mineralization processes in a hierarchical manner from geodynamic setting through province-through district-to deposit-scale. This mineral systems concept was first formulated by Wyborn et al. (1994) and championed by Knox-Robinson and Wyborn (1997) and Hronsky and Groves (2008), but it is only in the last decade that it has reached prominence as a critical approach in conceptual targeting (McCuaig et al., 2010; McCuaig and Hronsky, 2014; Hagemann et al., 2016; Huston et al., 2016; Wyman et al., 2016). The mineral systems model requires a fertile ore-component source in a suitable geodynamic setting with favourable linked lithosphere and crustal architecture for ore-fluid migration to a trap site, with suitable post-mineralization tectonic processes to ensure preservation (McCuaig and Hronsky, 2014). It is the multiplication effect of the conjunction of essential components of the mineral system (Fig. 1) that determines if an ore body forms and dictates its size and economic value (Megill, 1988). Based on these concepts and the evidence that ore-forming systems, like earthquakes, are rare events that have power-law distributions, Hronsky (2011) introduced the concept that large mineral deposits are examples of self-organised critical systems involving transfer of anomalously high energy and fluid fluxes into the crust. Wyman et al. (2016) and Hronsky (2019) have aligned this concept into the field of orogenic gold deposits, as discussed further below.

3. Evolution of models for orogenic gold deposits

The term orogenic gold deposit was defined by Groves et al. (1998), following Gebre-Mariam et al. (1995), as a coherent group of vertically-extensive, gold-only deposits that formed in broad thermal equilibrium with their wall-rocks from low-salinity H_2O–CO_2 ore fluids at crustal depths from 2 km to 15 km, and arguably up to 20 km (Groves, 1993; Kolb and Meyer, 2002; Kolb et al., 2005a, 2005b, 2015). Although this term is widely accepted (Goldfarb et al., 2001, 2005, 2014a; Bierlein et al., 2006), there is ongoing debate on the genesis of this deposit group.

Goldfarb and Groves (2015) provide an exhaustive review of these genetic models and the various geological, geochemical, isotopic and fluid-inclusion constraints on the component ore fluids and gold-related metals that formed orogenic gold deposits. All models depicted schematically in Fig. 2 are described and assessed in detail by Goldfarb and Groves (2015), who also provide exhaustive references to numerous individual examples.

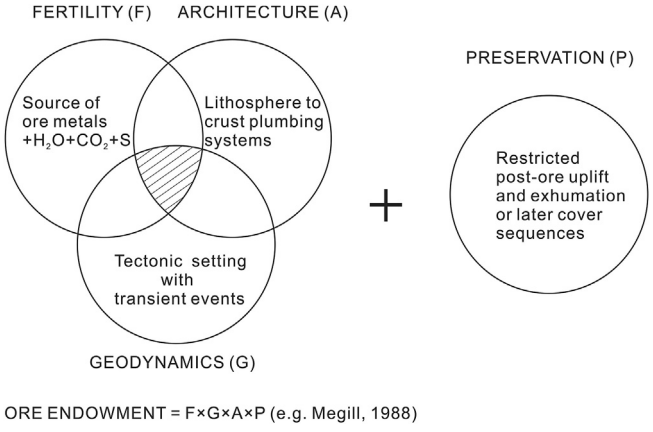

Fig. 1. Critical elements of a mineral system, with emphasis on orogenic gold. Adapted from McCuaig and Hronsky (2014).

3.1. Shallow crustal and magmatic-hydrothermal models

The models (Fig. 2a) shown to be less-viable by Goldfarb and Groves (2015) include early syngenetic-exhalative models which are inconsistent with field evidence that shows the deposits are structurally-controlled, syn- to late-metamorphic deposits with stratiform to stratabound BIF-hosted deposits formed by sulfidation of magnetite (Phillips et al., 1984). Similarly, meteoric fluid models are shown to be untenable because they are based on H and O isotope data largely derived from extraction of measured components from mixed primary and secondary fluid inclusions.

Early 20th century magmatic-hydrothermal models were re-emphasized for orogenic gold deposits by a number of authors (Fig. 2b). However, globally, granitic intrusions may be pre-, syn- or post-gold in the same terranes, or even absent in some, for example in the Otago gold province of New Zealand and in the Yukon. Where robust geochronological studies have been conducted, the gold deposits and proposed fertile granitic intrusions are not the same age, as summarized by Goldfarb and Groves (2015). In addition, the proposed parent granitic rocks have no consistent composition or oxidation state within or between terranes in contrast to other gold-bearing deposits (e.g., reduced IRGDs; Baker, 2002: oxidized porphyry Cu–Au; Hedenquist and Lowenstern, 1994). In some cases, lamprophyres and other more mafic intrusions have a similar age to the gold deposits (Vielreicher et al., 2010), but are volumetrically too minor to have provided the large volumes of fluids required to form the gold deposits. Therefore, magmatic-hydrothermal processes cannot explain the genesis of individual deposits let alone provide a universal mineral system model for orogenic gold formation, as eloquently argued by Wyman et al. (2016).

3.2. Crustal metamorphic models

The exclusion of the above models leaves metamorphic models as the only viable possibilities if a universal or near-universal model is sought for the genesis of orogenic gold deposits.

As Goldfarb and Groves (2015) argue, lateral secretion models (Boyle, 1979) are invalid due to the limited volume of metamorphic fluid and metals that could be generated together with the unlikely dominance of lateral flow. Models involving advection of mantle CO_2 through the lower crust to generate granulites and a CO_2-rich pseudo-metamorphic fluid are invalidated by lack of universal associations between granulites and gold, too low CO_2 contents of fluid inclusions, and available carbon isotope data.

Such logical arguments have led to general acceptance of a model that promotes metamorphic devolatilization of largely supracrustal rocks within the continental mid crust under greenschist-to amphibolite-facies conditions. This model emphasises gross upwards advection of resultant metamorphic fluid and metals to the depositional site of orogenic gold mineralization at higher crustal levels (summarized by Goldfarb et al., 2005; Phillips and Powell, 2010; Tomkins, 2010; among many others). This crustal metamorphic model is the only one of those discussed above for mesozonal to epizonal (terminology of Gebre-Marium et al., 1995)

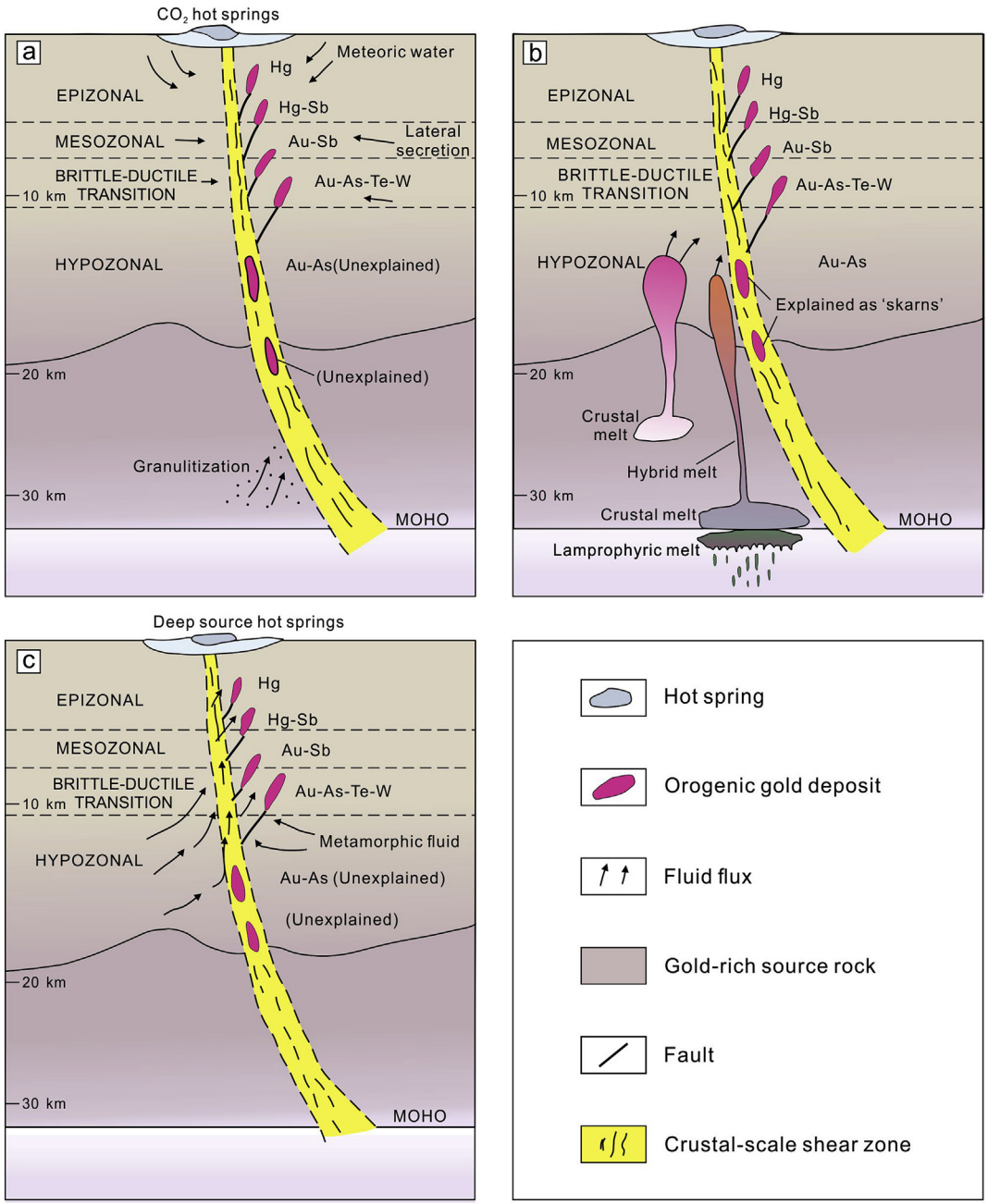

Fig. 2. Schematic representation of ore-fluid source models for orogenic gold deposits: (a) Invalid shallow crustal meteoric or metamorphic models and granulitization models; (b) non-unifying magmatic-hydrothermal models; (c) generally accepted supracrustal metamorphic models. Adapted from Groves and Santosh (2016).

orogenic gold deposits that potentially could provide a universal model to explain their extraordinary longevity throughout Earth history (Goldfarb et al., 2001). Its main strengths are that it requires no specific association with host rock units, as most are mineralized in gold provinces globally, nor with any specific intrusion type. It also complies with the broadly late-metamorphic and late-deformational timing of gold deposition for most deposits, and the stable and radiogenic isotope data that are internally ambiguous but collectively suggest long and complex continental fluid pathways (Ridley and Diamond, 2000). The typical low-salinity H_2O–CO_2 ($\pm$ CH_4, N_2) fluid is also that expected from metamorphic devolatilization of supracrustal rocks (Fyfe et al., 1978).

In such a metamorphic model, gold rich fluids would have to been derived from different source rocks at different times in Earth history (Goldfarb and Groves, 2015) within different tectonic terranes where anomalous heat flow and consequent regional metamorphism was caused by a variety of crustal- to mantle-related processes (Goldfarb et al., 1986). Despite such high variability, it is important to recognise that gold deposition globally appears to be broadly coincident with a short-duration change in far field stress. This resulted in a transition in deformation from compression to transpression, more rarely transtension, during accretion (Goldfarb et al., 1988) with concomitant uplift and lowering of lithostatic pressure (Groves et al., 1987; White et al., 2015).

3.3. Weaknesses of the crustal metamorphic model

Despite the obvious strengths of many aspects of the crustal metamorphic model, there are several weaknesses, most obviously for Precambrian deposits, but also for an increasing number of Phanerozoic deposits, particularly in China. These are outlined in detail by Groves et al. (2019) and are only briefly summarized here.

The most obvious, potentially insurmountable, problem for the

crustal metamorphic model as applied to Precambrian, particularly Archean, terranes is the occurrence of a significant number of deposits world-wide in mid- to upper-amphibolite facies domains, as demonstrated by Kolb et al. (2015) among others. Importantly, these hypozonal deposits have alteration assemblages that formed under similar P-T conditions to the metamorphosed host rocks (Colvine et al., 1988; Knight et al., 1993; McCuaig et al., 1993; Neumayr et al., 1993; Bloem et al., 1994; Miller and Adams, 2013) with structural style varying in sympathy with the P-T conditions of alteration assemblages (Groves, 1993, Fig. 3). Hence, the fluid source must have been deeper than the 15 km (possibly up to 20 km) depth of deepest orogenic gold deposit formation, not from devolatilization during amphibolite-facies metamorphism as proposed in the crustal metamorphic model. Additional evidence for a deep source is also provided by lead isotope evidence from the giant Neoarchean Eastern Goldfields Province of the Yilgarn Craton gold province of Western Australia (Browning et al., 1987; McNaughton et al., 1993). Here, lead isotope ratios from the orogenic gold deposits reflect the age and composition of the basement rocks to the supracrustal greenstone belts, implicating a deep source for the auriferous ore fluids. In addition, it is also uncertain whether the dominantly mafic rocks of most Precambrian greenstone belts can be a source for all gold-related metals during their metamorphic devolatilization (Pitcairn et al., 2015).

Finally, recent research on multiple sulfur isotopic compositions of Neoarchean orogenic gold deposits in Western Australia (Fig. 4) demonstrates that neither local supracrustal rocks nor granitic intrusions can have supply the majority of sulfur for deposition of gold-related sulfides in the deposits. The data from Selvajara et al. (2017) and LaFlamme et al. (2018) show that the sulfur for the auriferous fluids was derived from a reservoir that was homogenized a depth and contained recycled MIF-S that was sourced from an Archean sediment reservoir other than that in the greenstone belts themselves: that is, a sub-crustal source.

Phanerozoic orogenic gold deposits in general fit the crustal metamorphic model well in that the majority of significant mesozonal to epizonal deposits are recorded to be in greenschist-facies domains, mainly in turbidite sequences (Goldfarb et al., 2005). Pitcairn et al. (2006) demonstrate it is feasible to release significant Au, As, Bi, Sb, Te and W, the major ore elements, from such sequences during greenschist- to amphibolite-facies metamorphism. However, there are exceptions as for Precambrian equivalents (Fig. 5).

For example, the late Carboniferous to early Permian (315–285 Ma) gold deposits of the Variscan belt in the Massif Central of France (Goldfarb et al., 2001) include hypozonal deposits in the amphibolite-facies domains of the Saligne (4 Moz gold) and St-Yreix (1.3 Moz gold) districts (Bouchot et al., 2005).

Other exceptions include some ~370 Ma lode gold deposits hosted in turbidite sequences in the Paleozoic Meguma Group, Nova Scotia, Canada (Kontak et al., 1990; Ryan and Smith, 1998). Although most gold deposits are sited in greenschist-facies domains, several, including Beaver Dam and Cochrane Hill, are located in amphibolite-facies domains and are interpreted by Kontak et al. (1990) to be derived from a sub-crustal fluid source released during regional doming.

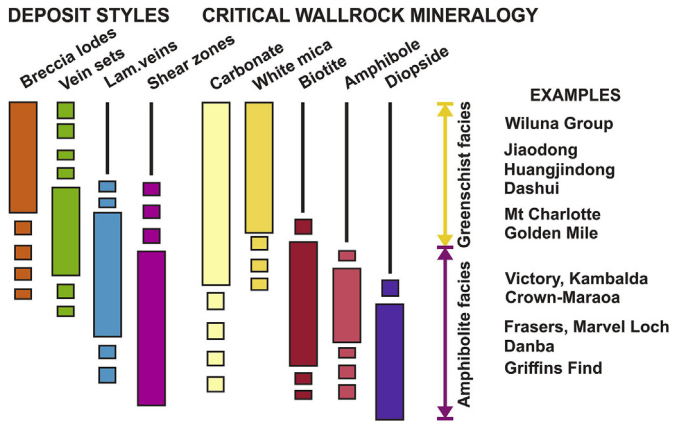

Fig. 3. Schematic diagram showing concomitant changes in structural style and alteration assemblages for orogenic gold deposits. Pyrite dominates in low metamorphic grade domains whereas pyrrhotite and loellingite dominate in higher metamorphic grade domains. Simplified from Groves (1993).

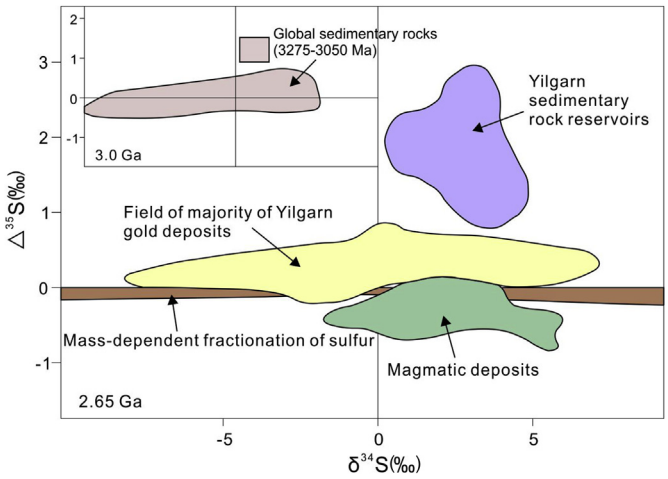

Fig. 4. Summary of multiple sulfur isotope compositions of Neoarchean gold deposits in the Yilgarn Block of Western Australia compared to possible Yilgarn sedimentary reservoirs and magmatic reservoirs. The field of the great majority of Yilgarn orogenic gold deposits is generalized from Salvaraja et al. (2017) and LaFlamme et al. (2018): outliers that fall into the magmatic field are mainly from the deposits in the Kalgoorlie goldfield. Adapted from Groves et al. (2019).

The recently recognized hypozonal orogenic gold deposit at Danba (Zhang et al., 2018) is located in a poorly-documented gold province on the north-western margin of the Yangtze Block, China (Fig. 5), which is dominated by a >1000 km Mesozoic domal domain along the Longmenshan thrust nappe belt. It is clearly a hypozonal orogenic gold deposit hosted in a broadly strata-bound ductile-brittle shear zone with high-T proximal alteration assemblages of biotite-amphibole-plagioclase and ore assemblages dominated by pyrrhotite, but with a strong association between gold and bismuth tellurides. Danba clearly represents a Lower Jurassic high P-T orogenic gold deposit that formed during post-peak amphibolite-facies metamorphic retrogression.

Additionally, equivalent to the Neoarchean deposits of Western Australia, orogenic gold deposits throughout the Paleozoic of Ireland (Standish et al., 2014) are characterized by highly variable lead signatures. These reflect many different lithologies, including the basement, thus indirectly indicating a source external to the hosting supracrustal sequence.

4. Deposits on north China and Yangtze Block margins: the game changers

In conjunction with the issues discussed above, recent interest and documentation of Chinese gold deposits, particularly those close to the margins of the North China and Yangtze Blocks, has effectively seen the demise of the crustal metamorphism as a universally viable process for generation of orogenic gold deposits.

The giant Jiaodong gold province (Fig. 5) in the eastern half of the North China Block (Deng et al., 2003; L. Li et al., 2015; N. Li et al., 2015a, 2015b; Song et al., 2015; Yang et al., 2015, 2016; Yang and Santosh, 2015, 2020) has been the major game changer in the search for a universal model. It represents a region of major lithospheric erosion of originally thick buoyant Archean SCLM (Griffin et al., 1998; Santosh, 2010a, 2010b), caused by anomalously complex Mesozoic slab subduction pene-contemporaneously from the north, south, and east. This led to slab devolatilization, consequent melting, and associated voluminous granitic magmatism (Windley et al., 2010). The associated Yanshanian

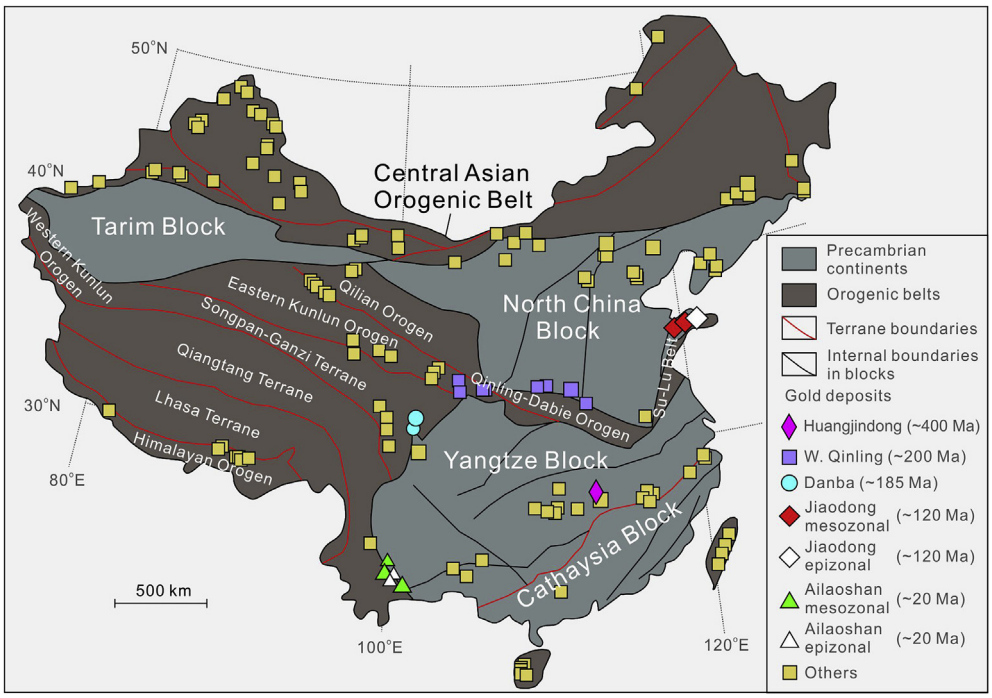

Fig. 5. Distribution of hypozonal orogenic deposits in amphibolite-facies domains and enigmatic deposits where timing negates a supracrustal metamorphic source in China. Base map adapted from Goldfarb et al. (2019).

(Jurassic–Cretaceous) orogeny, that occurred within the de-cratonized North China Block, was typified by basement uplift, regional extension, ca. 165–90 Ma granite intrusion, and ca. 120 Ma gold formation (Zhang et al., 2020) within the eastern margins of this highly modified cratonic basement (Goldfarb and Santosh, 2014; Yang and Santosh, 2014). The timing of gold mineralization (Zhang et al., 2020) argues against a magmatic-hydrothermal fluid model, and the Precambrian high-grade metamorphism of the basement rocks clearly invalidates a crustal metamorphic-devolatilization model for the gold event. Despite this, the widespread gold episode correlates with changing far-field stresses and plate reorganizations and the Jiaodong deposits have generally been classified as orogenic gold deposits (Wang et al., 1998; Goldfarb et al., 2001, 2005; Yang et al., 2015a, 2016a). They show a clear structural control along regional faults (Deng et al., 2018, 2019), and ore and wallrock-alteration mineralogy, fluid inclusion compositions and stable isotope chemistry are similar to more typical orogenic gold deposits, particularly of epizonal type (Yang et al., 2015, 2016).

The Tertiary gold deposits in northwestern Mexico along the Mega-shear Zone in the Proterozoic–Phanerozoic terranes of northern Mexico (Iriondo, 2001; Goldfarb et al., 2007) are hosted in reactivated high-grade Proterozoic basement in extensional structures within metamorphic core complexes and appear to be analogues of the Jiaodong deposits.

Other Chinese gold deposits on the margins of the North China and Yangtze Blocks present similar, although more subtle, problems. For example, Goldfarb and Groves (2015) indicate significant timing problems for a crustal metamorphic model to form the mesozonal to epizonal orogenic gold deposits in the potentially giant Triassic Qinling gold province (Chen et al., 2008). This region marks the closure of the northernmost paleo-Tethys sea and the tectonic suturing of the Yangtze and North China Blocks (L. Li et al., 2015; N. Li et al., 2015a, b; Dong and Santosh, 2016). Recent research on the large Yangshan, Mian-Lue-Ning and Manaoke orogenic gold districts in the province (Li et al., 2018) confirm that, at the time of regional metamorphism, there were no previously un-metamorphosed voluminous source rocks that could have experienced fluid and metal liberation during amphibolite facies metamorphism, implicating an external deeply-sourced fluid.

The Huangjindong goldfield, hosted in Neoproterozoic slate, formed in a transpressional regime with deposits linked to the crustal-scale Chang-Ping Fault in the Jiangnan Orogen, Hunan Province, China. The mesozonal orogenic gold deposits are dominated by structurally-controlled auriferous arsenopyrite-pyrite-quartz-(scheelite) veins and quartz-rich breccias that overprint earlier barren quartz veins (Zhang et al., 2019a). Geological and isotopic data indicate that the ore-forming components had a metamorphic source. Importantly, however, the host Neoproterozoic slate exposed over the entire province has only undergone greenschist-facies metamorphism, and so cannot be an effective, dominant source of crustal metamorphic ore fluid or metal (Zhang et al., 2018), again implicating a deeper, external source.

A series of Upper Oligocene and Lower Miocene orogenic gold deposits, including the mesozonal lode-type Daping and epizonal disseminated-style Chang'an, Zhenyuan and Jinchang gold deposits, are distributed along the western margin of the NNW-trending Ailaoshan shear zone between the South China and Indochina Blocks in southeastern Tibet (Deng and Wang, 2016). Paleomagnetic data from mineralized rocks indicate a very late timing of gold mineralization following termination of the dominant shearing and fault displacement at ca. 21 Ma, arguing against a crustal source of metamorphic ore-fluid (Gao et al., 2018). Integration of C–O and He–Ar isotope compositions from ore-related carbonates and pyrites, respectively, in the deposits indicate a fluid source with both mantle and crustal components, and timing incompatible with regional metamorphism, suggests a deep sub-crustal source for the Ailaoshan deposits (Wang et al., 2019).

5. A coherent mineral system model for orogenic gold deposits

As argued succinctly by Wyman et al. (2016), a mineral systems model for orogenic gold deposits must represent a single coherent model capable of explaining the genesis of all deposits within the group.

5.1. *Fertility parameter*

From the discussion presented above and those developed by Wyman et al. (2016), there are an increasing number of orogenic gold deposits

that cannot be derived from magmatic-hydrothermal or crustal metamorphic fluid sources. Hence, for a coherent model, the fertility parameter of the mineral system must be represented by a sub-crustal H_2O–CO_2 S-bearing fluid containing dissolved Au and associated metals such as Ag, As, Bi, Sb, Te and W. The question then arises as to the nature of the sub-crustal source. As discussed in detail by Goldfarb and Groves (2015), there are few unequivocal indications of this precise fluid or metal source from fluid inclusion, stable isotope or radiogenic isotope data. This is because most data do not represent the original fluid and metal source, but rather the modification of that source by reactions along the long crustal pathways traversed by the fluids as they migrate towards gold depositional sites (Ridley and Diamond, 2000). The only obvious universal constraints are that the original fluid was almost certainly near-neutral and reduced (Goldfarb and Groves, 2015), although S isotope ratios of ore-related sulfides can, in some instances, discriminate between alternative sources (Wang et al., 2019). Thus, the ultimate sub-crustal source of fluid and metals must largely be deduced, as discussed below, through logical interpretation of geological constraints based on factors such as geodynamic setting and tectonic timing.

5.2. Geodynamic parameter: normal convergent margins

To resolve this question, the nature of geodynamic setting, the second component of the mineral system (Fig. 1), must be addressed. It is widely accepted that orogenic gold deposits are inevitably formed in accretionary or, less commonly, collisional tectonic environments related to subduction (Goldfarb et al., 2001, 2005), and not in other types of metamorphic belts, indicating that convergent margins are the critical dynamic setting. Such a geodynamic environment can explain the conjunction of apparent late- to post-metamorphic timing in host sequences precisely at the time that a change in far-field stresses promoted a change from compression, as represented by the structures and metamorphic fabrics in the host rocks, to transpression or transtension, as demonstrated by the geometry of the orogenic gold ore-bodies (Groves and Santosh, 2015). This implicates a fundamental relationship to a change in plate motion on the whole-Earth scale. As discussed by Seno and Kirby (2014), this might be brought about by the cessation of subduction, perhaps due to collision with a basement block, such as the Selwyn Block in the Victorian Goldfields of eastern Australia (Moresi et al., 2014), or stalling of the slab during subduction, particularly flat subduction (Wyman et al., 2008; Wyman and Kerrich, 2010). These tectonic processes could result in a change of stress regime as plates were reorganised with subsequent switchover from compression to transpression.

In this geodynamic setting, the only conceivable sub-crustal source of fluid and metals is subducted oceanic crust and an overlying sediment wedge (Goldfarb and Santosh, 2014; Goldfarb and Groves, 2015; Groves and Santosh, 2016; Wyman et al., 2016). Devolatilization of a subducted slab can result in extensive upward fluid-flux along slab-mantle boundaries (Sibson, 2004; Peacock et al., 2011; Katayama et al., 2012) into fore-arc or accreting terrane margins. At this stage, the oceanic slab will devolatilize, together with its overlying pyrite-bearing oceanic sediment wedge. The latter is important because gold and related elements such as Ag, As, Bi, Sb and Te can be released to the fluid via breakdown of sedimentary pyrite to pyrrhotite (Large et al., 2009, 2011; Steadman et al., 2013). Such fluids can be then transported from the mantle to crustal levels in lithosphere- to crustal-scale fault zones as shown by radiogenic isotope, halogen and noble gas data from the San Andreas Fault system (Kennedy and van Soest, 2007; Pili et al., 2011) and the Karakorum Fault zone (Klemperer et al., 2013).

Over-pressured fluids (Sibson, 2013) as injection-driven seismic swarms (Cox, 2016) could then migrate up-dip, channelling into crustal-scale fault zones at higher crustal levels to eventually deposit orogenic gold deposits at even shallower levels in lower-order structures (Breeding and Ague, 2002; Hyndman et al., 2015). A schematic model, adapted from the Goldfarb and Santosh (2014) and Groves et al. (2019) models is presented in Fig. 6.

This model can also elegantly explain the sympathetic relationship between the S isotope compositions of gold-related sulfides and the S isotope composition of seawater sulfate at the period of formation of most gold deposits (Fig. 7). This is because sediments transported down the subduction zone would have been derived via reduction of seawater sulfate. In addition, the richness of Neoarchean orogenic gold deposits could at least be partly explained by the occurrence of the most gold-enriched sedimentary/diagenetic pyrites at this time in Earth history (Large et al., 2014). The higher CO_2 content of the Archean ore fluids could also be explained by a greater degree of carbonation in Archean oceanic rocks due to a combination of more-susceptible high-MgO basalts and lack of CO_2 sinks (Groves and Santosh, 2016: fig. 4).

5.3. Geodynamic parameter: convergent margins adjacent to continental blocks

Several of the Chinese orogenic gold provinces are sited on the margins of, or adjacent to, the continental North China and Yangtze Blocks. In their geodynamic model for the well-documented Jiaodong deposits, Goldfarb and Santosh (2014) suggested that the auriferous fluids could be either derived directly from the subduction zone, as implied in Fig. 6, or indirectly from the mantle lithosphere wedge that had been fertilized and metasomatized by fluids derived from that subduction zone. Subsequent geochemical and isotopic syntheses by Deng et al. (2019) have not only supported the latter model but shown, particularly on the basis of discrepant Neoproterozoic S isotope compositions of gold-related sulfides, that mantle-lithosphere metasomatism was related to a much earlier subduction event.

As discussed above, the timing of generation of gold mineralization for the Danba hypozonal orogenic gold deposit (Zhang et al., 2018) and for the Ailaoshan mesozonal to epizonal orogenic gold belt (Wang et al., 2019) is incompatible with direct derivation from devolatilization of subduction-related sediment wedges. The belts hosting both groups of deposits are anomalous in terms of their tectonic history and zones of metamorphic core complexes, suggesting anomalous crustal heating and extension. In both cases, there is evidence of underlying mantle-lithosphere that was metasomatized during devolatilization related to an earlier subduction event (Zhou et al., 2002; Zhao and Zhou, 2008). As for the Jiaodong deposits, this has now been confirmed for Danba from geochemical and isotopic data on the gold ores, particularly the S isotope compositions that are incompatible with derivation from sedimentary sulfides subducted at the time of gold mineralization (Wang et al., 2019). Gold enrichment is also confirmed by studies of mantle xenoliths which show enrichment up to three times greater than elsewhere for mantle lithosphere beneath the North China Craton (Saunders et al., 2018). The only viable model for ore-fluid generation is devolatilization of this metasomatized mantle lithosphere by thermal anomalies channelled towards craton or other lithosphere margins (Begg et al., 2009), with subsequent advection up crustal-scale faults adjacent to the gold districts, as shown schematically in models in Deng et al. (2019), Wang et al. (2019a, 2019b), and Zhao et al. (2019), and Yang and Santosh (2020). Similar models have also been discussed more broadly by Bierlein and Pisarevsky (2008), de Boorder (2012), Hronsky et al. (2012), Webber et al. (2013) and Wyman et al. (2016), among others.

The mechanisms for migration into the crust by such anomalous fluids created through devolatilization of metasomatized mantle lithosphere have been rarely addressed (Kennedy et al., 1997; Burnard and Polya, 2004; Finlay et al., 2010; Klemperer et al., 2013), with seismic pumping along crustal-scale faults as one logical mechanism (Cox, 2016). Rapid passage of such deeply-sourced ore fluid through faults with zones of local water saturation may be the mechanism to prevent the ore fluids from being consumed through partial melting to produce magmas in a more normal scenario (Schrauder and Navon, 1994; Bureau and Keppler, 1999; Klein-BenDavid et al., 2011; Rospabé et al., 2017).

A schematic diagram showing both the direct fluid-derivation

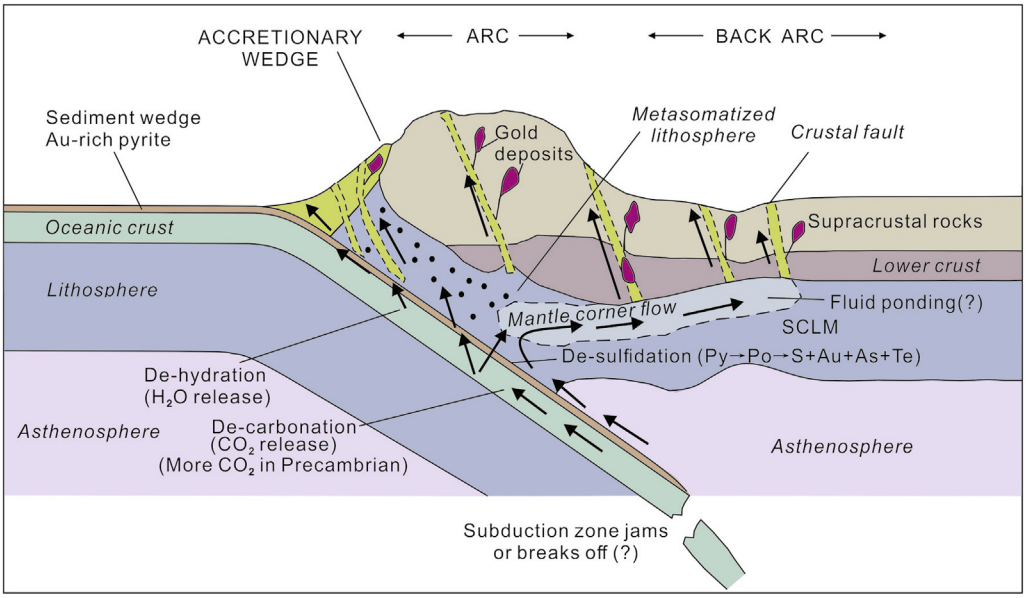

Fig. 6. Schematic representation of subduction-based model for ore-fluid source for orogenic gold deposits globally. Adapted from Groves et al. (2019).

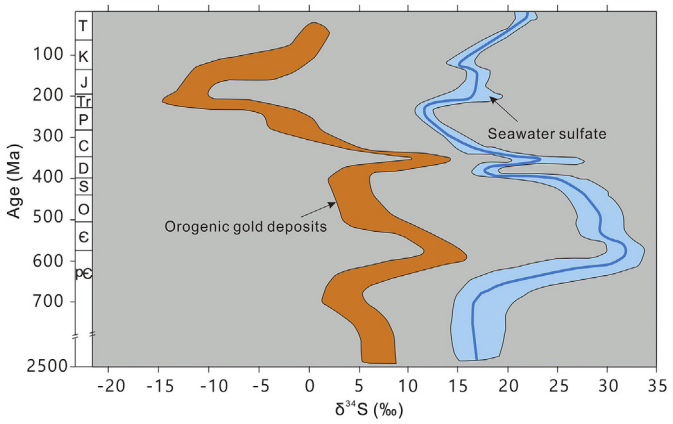

Fig. 7. Sulfur isotope compositions of most orogenic gold deposits show a consistent relationship with those of seawater sulfate at the time of gold mineralization. Note that there are exceptions for some Chinese deposits discussed in the text. After Goldfarb et al. (1999).

subduction model and the indirect fluid-derivation model from metasomatized mantle lithosphere is shown in terms of a self-organising system in Fig. 8 as a prelude to discussion below of architecture in the orogenic gold mineral system.

5.4. Architecture parameter: fluid plumbing system

For the mineral system orogenic-gold model(s) defined above, a favourable whole-lithospheric architecture is required, particularly to allow for focused propagation of auriferous fluids to the surface (McCuaig and Hronsky, 2014). In agreement, most authors (see summaries in Groves et al., 2000; Goldfarb et al., 2005; Robert et al., 2005), agree that the first-order control on world-class orogenic gold districts is their location adjacent to crustal-to lithospheric-scale fault or shear zones at the province scale (Fig. 2). These structures are commonly marked by anomalous concentrations of lithosphere-sourced lamprophyre dykes or felsic-intermediate intrusions with mantle source components (Witt et al., 2013) that indicate a deep lithospheric connection for fluid conduits (Perring et al., 1987; Rock et al., 1989). The first-order faults are most highly endowed where they are intersected by high-angle accommodation structures (Hronsky et al., 2012; Goldfarb and Groves, 2015; Groves et al., 2016; Groves and Santosh, 2016; Wyman et al., 2016 and earlier references within). Less-endowed orogenic gold provinces (e.g., Zimbabwe gold provinces; Klondike province; Seward Peninsula of Alaska) lack these first-order structures and associated lamprophyres.

The distribution of gold mineralization proximal to major lithosphere-scale conduits is predominantly controlled by second-order, belt-scale structures that act to focus fluid flow. These generally propagate along lines of weakness, such as pre-existing reactivated thrust faults or contacts between lithological units with high competency contrasts. Mineralization at the deposit scale is focussed by third-order, physical throttles and host rocks that act as physical and chemical traps to promote the precipitation of minerals from auriferous fluids (Joly et al., 2010; McCuaig et al., 2010; McCuaig and Hronsky, 2014; Hagemann et al., 2016). Common structural traps include tight, faulted antiforms, intersections between strike-extensive shear zones and high-angle fault corridors, commonly at jogs in the former, irregular sheared margins of small granite or other intrusions and triple-point junctions between adjacent intrusions (Groves et al., 2018). Important chemical traps include fractured iron-rich host rocks and carbonaceous sedimentary units (Goldfarb and Groves, 2015).

There is also the requirement for a cap on the hydrothermal system to effectively impound fluid flux within the permeable trap zone. For Archean and Paleoproterozoic orogenic gold systems in particular, this is normally provided by relatively impermeable metasedimentary sequences that overlie more-permeable fractured volcanic sequences in greenstone belts (Groves et al., 2003). For younger systems, the controls may be more subtle variations in the thickness and/or rock strength of turbidite sequences, or thrusts that emplace less permeable sequences over trap rocks, as for example in Nevada for Carlin-type deposits (Cline et al., 2005).

As these structure-host rock geometries are the most critical exploration criteria at the district scale, they are discussed in more detail below in sections dealing with critical exploration parameters based on the mineral system model.

5.5. Preservation parameter

For all mineral deposits, preservation is as important as formation in dictating the distribution of deposits through time (Groves et al., 2005b). For many mineral deposit types formed at shallow crustal levels, uplift,

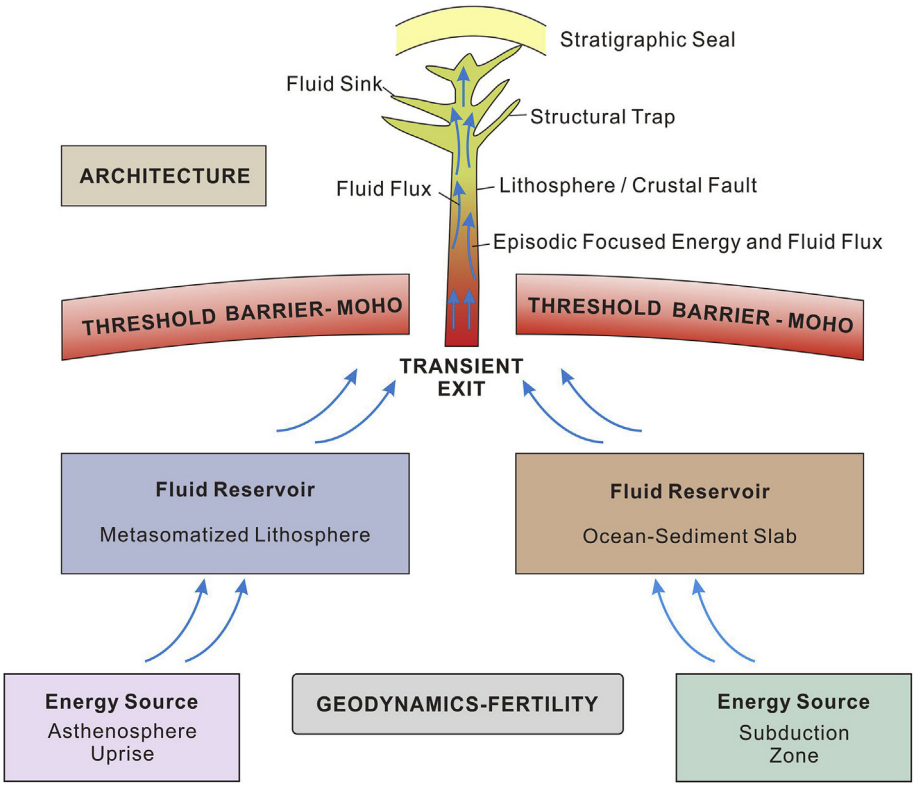

Fig. 8. Schematic self-organising critical orogenic gold mineral system showing alternate fertility sources that have the same basic architecture parameters. Adapted from Wyman et al. (2016).

exhumation and erosion dictate a relatively short geological lifetime. However, orogenic deposits are anomalous hydrothermal gold deposits in that they formed at crustal depths >2 km and mostly >5 km (Groves, 1993; Goldfarb et al., 2005), and have better preservation potential because of their late-orogenic timing (Goldfarb et al., 2001: figs. 3 and 4). Precambrian deposits were preserved because they formed just prior to cratonization with the development of thick buoyant sub-continental lithosphere keels beneath them (Griffin et al., 1998, 2013; Wyman and Kerrich, 2002; Groves et al., 2005a). It is only in the Mesoproterozoic and early Neoproterozoic that orogenic deposits are essentially absent in anomalous exhumed high-grade metamorphic roots to orogenic belts globally (Goldfarb et al., 2001).

6. Introduction to critical mineral-system-based exploration criteria

The critical components of the mineral-system orogenic-gold model (Fig. 1) are discussed in logical order from Geodynamics to Fertility to Architecture to Preservation and summarized in a series of tables. For the orogenic model, Fertility is intimately linked to Geodynamics, so these are grouped together in Table 1. The geodynamic setting can be identified by critical parameters, most of which, in practise, can only be recognized via geological proxies and geophysical responses. Architecture can be viewed pragmatically at province and district to deposit scales, as shown on Tables 2 and 3, respectively. The genetic processes can be identified by geological parameters, but, in practise, these can often only be identified by geological proxies or by geophysical or geochemical signatures, as discussed below.

7. Geodynamics and fertility exploration factors

As discussed above, the critical fertility factor is related to the subduction of an oceanic slab and overlying sediment wedge that can provide fluid, sulfur, gold and other ore metals to the orogenic gold system (Figs. 6 and 8). As subduction is effectively linked to convergent margin geodynamic settings, these must be identified as crucial terranes or provinces within which to target gold exploration. A caveat is that Mesoproterozoic to early Neoproterozoic terranes are likely to be poorly endowed relative to all other periods of Earth history. Many convergent margin terranes will have their fertility marked by significant gold occurrences as gold prospecting has been a global occupation for centuries. However, a consistent assessment of past convergent margin settings may open up new exploration spaces in more remote regions.

In this context, it is useful to consider the modern concepts on convergent margins and related processes, particularly since oceanic subduction along convergent margins is the major site of building and recycling continental crust (Stern, 2011; Straub and Zhellmer, 2012). Convergent margin processes exert a significant control over the nature and style of metallogeny (Groves et al., 2019). The evolution and preservation of continents and their mineral resources through time are largely controlled by the processes of creation and destruction of continental crust in subduction zones. Tectonic erosion along convergent margins by down-going oceanic plates, including arc subduction and sediment subduction, results in the destruction of continental crust, erosion of craton roots, and modification of the subcontinental lithospheric mantle, thus significantly influencing the geochemical cycle of the Earth in general (Yamamoto et al., 2009; Vannucchi et al., 2016). Deep subducted material accumulates at the mantle transition zone or over the core-mantle boundary which is recycled and incorporated into rising plumes, representing major pipes that transfer elements and volatiles to higher levels in the crust (Santosh et al., 2009). The magmatic, metamorphic and metasomatic 'factories' operating in subduction zones provide potential and diverse pathways for element transfer (Maruyama et al., 2009), building deep-seated archives of metals which contribute to the formation of major mineral deposits (Yang and Santosh, 2020).

Convergent margin tectonics is considered to be responsible for building the major global types of orogenic belts that are termed accretionary and collisional orogens (also known as Pacific-type and

Table 1
Recognition of prospective convergent margin settings with fertile fluid source and lithosphere-scale fluid plumbing system.

SETTINGS	CRITICAL PARAMETER	GEOLOGICAL PROXY	GEOPHYSICAL RESPONSE
Subduction in Normal Convergent Margins (Archean-Tertiary)	Lithostratigraphic sequences corresponding to arc and accretionary sequence indicating geodynamic setting	Arc-type mafic-intermediate-felsic volcanic suites. Thick turbidite sequences. Accreted Ocean Plate Stratigraphy. Greenstone belts (Precambrian)	Variable, normally subtle, aeromagnetic and seismic signatures
	Mantle- to crustal-derived granitic intrusions, remnants of mafic island arc crust	Abundant arc-related and crustal-derived granitic intrusions with lesser hybrid intrusions and lamprophyres	Normally ovoid negative or mildly positive aeromagnetic anomalies with negative gravity
	Strong metamorphic gradients dominated by low-P Barrovian metamorphic terranes	Sub-greenschist to amphibolite-facies domains. Granulites rare in Phanerozoic terranes and blueschists absent in Archean terranes	Strong aeromagnetic gradients defining metamorphic boundaries
	Classic deformation sequence of D_1 to D_4 with late orogenic collapse	Early extension and rifting. D_1 thrusting, D_2–D_3 upright folding and thrust reactivation D_3–D_4 oblique-slip shearing/faulting	Aeromagnetic linears define major structures
	Accretion: suspect terranes	Juxtaposition of sequences of different age and provenance. VMH deposits may be accreted	Large-scale 'stripes' of aeromagnetic and gravity signatures
Subduction/Collision on Lithospheric, commonly Cratonic Margins (Mostly Phanerozoic)	Fragmented craton margins	High-grade metamorphic rocks juxtaposed against lower metamorphic grade rocks. Phanerozoic shelf-facies sedimentary sequences along margin	Gravity, seismic and magneto- telluric sections reflect fragmentation at boundaries defined by aeromagnetic linear boundaries
	Metasomatized mantle lithosphere	Distinctive hybrid intrusions. Metasomatized mantle xenoliths	
	Very complex structural history	Commonly complex fold-fault patterns, including late-orogenic metamorphic core complexes	Complex aeromagnetic and gravity patterns
	Complex array of igneous intrusions	Intrusions mainly crust-derived external to craton with hybrid intrusions in fragmented craton and overlying sedimentary sequences	Complex aeromagnetic and gravity patterns with strong gradients

Himalayan-type; Maruyama et al., 1996; Cawood et al., 2009; Santosh et al., 2009). The major components resulting from the two types of orogeny are distinct. The hallmark of accretionary-type orogeny is an accretionary complex comprising oceanic materials such as MORB, seamounts, Ocean Island Basalt (OIB), carbonates and deep-sea sediments. Commonly, an extensive batholith belt forms on the continental side and fore-arc basins are formed in between. In collisional-type orogens, passive continental-margin sequences dominate, with the orogenic core composed of regional metamorphic belts, and a collisional suture zone which preserves the remnants of oceanic rock sequences. Accretionary orogens have been further grouped into retreating and advancing types (Cawood et al., 2009). The modern western Pacific provides an example of a retreating orogen with a characteristic back-arc basin, whereas the Andes with its foreland fold and thrust belt, with crustal thickening, is considered to be an advancing orogen. Accretionary orogens mark the major sites of consumption and reworking of continental crust, and are therefore important in understanding the evolution of continental crust and its resources. Since collisional orogens are the end product of accretionary orogeny, involving extensive subduction of oceanic lithosphere, the Himalayan-type collisional orogens also commonly incorporate the imprints of accretionary-type sequences. One of the best examples of a protracted history of subduction and accretion leading to final collision is provided by the Central Asian Orogenic Belt, considered as the world's largest Phanerozoic accretionary orogen, where diverse types of precious- and base-metal mineral deposits and major metallogenic belts were created during the multiple subduction-accretion-collision cycle (Goldfarb et al., 2014; Xiao et al., 2015).

One of the useful geological tools to distinguish extinct convergent margins from surface geology is the recognition of Ocean Plate Stratigraphy (OPS). The OPS has been defined as the original composite stratigraphic succession of the ocean floor which is incorporated in an accretionary complex and can be considered as the travelogue of an oceanic plate from mid oceanic ridge to subduction zone (Matsuda and Isozaki, 1991; Safonova et al., 2009; Santosh, 2010a, 2010b). A typical OPS sequence, accreted on to land, would thus be a sequence of MORB, chert, OIB and trench sediment (Isozaki et al., 2010). Identification of OPS has been also described from Precambrian terranes in recent studies (Kawai et al., 2009), including evidence from major suture zones associated with the assembly of Proterozoic supercontinents (Santosh et al., 2009). Ocean plate stratigraphy is thus a potential geological tool to identify subduction-accretion-collision tectonics, and also aids in characterizing convergent margin processes through time.

In Table 1, the convergent margin settings are broadly subdivided into those where normal accretionary processes operate and continental margins are only factors in the far back-arc and those, normally with late collisional tectonics, in which craton or other lithosphere margins play an important role during and after compressional orogenesis.

In the former, a combination of arc-type mafic-intermediate-felsic volcanic sequences and thick turbidite sequences are the critical

Table 2
Architecture 1. Critical parameters of the sub-crustal mineral-system orogenic-gold model at the province scale: assessment of subduction-related processes and source of fluid and ore components.

PROCESS	GEOLOGICAL PARAMETER	GEOLOGICAL PROXY	GEOPHYSICAL/GEOCHEMICAL RESPONSE
Thermal energy to drive sub-crustal mineral system	Heat from igneous intrusion Metamorphic gradients	Both crustal and mantle-derived intrusions Low-P metamorphic facies	Strong to weak ovoid aeromagnetic anomalies dependant on the nature of lithostratigraphic sequences and their metamorphic grade
Fluid flow from below MOHO into crust	Lithosphere- to crustal-scale plumbing systems	>100 km long fault of shear-zone (commonly with lamprophyres) within low-strain rock sequences with well-preserved structures and textures	Focussed, widely-spaced >100 km long aeromagnetic texture. Vertical structures defined by magneto-telluric sections
Gold-bearing fluid flow from sub-crustal sources	Anomalous metal enrichment in permeable zones	Anomalous metal enrichment along >100 km long shear zones	Linear multi-element (Ag, As, Au, Bi, Hg, Sb, Te, W) soil or rock-chip anomalies
Uplift to lower lithostatic pressures	Major vertical displacement of lithostratigraphic successions	Late conglomerate basins juxtaposed against lower rock units, particularly for Precambrian greenstone belts	Strong aeromagnetic and gravity contrasts at district scale

Table 3
Architecture 2. Critical parameters of the sub-crustal mineral-system orogenic-gold model at the district to deposit: assessing suitable thermal energy and fluid plumbing outlined at province scale in Table 2.

GENETIC PROCESS	GEOLOGICAL PARAMETER	GEOLOGICAL PROXY	GEOPHYSICAL/GEOCHEMICAL RESPONSE
Focussed fluid infiltration to suitable structural sites	High damage zones in second -or third-order faults adjacent to first-order faults	Jogs representing 10°–30° angular variations from the mean strike of first-order faults	Change in strike of regional aeromagnetic linears. More resistive zones (?)
	Cross faults that accommodate the high damage-zone jogs	Arrays of cross faults at approximately 70° to the second- or third-order faults	Arrays of aeromagnetic linear zones at high angle to the more continuous regional linear zones
	Fluid infiltration due to rotation of blocks between faults with the same kinematics	Complexity of structure at fault intersections	Local non-linear aeromagnetic patterns
	Metal enrichment in fluid plumbing systems	Alteration zones near fault intersections	Gold and related elements (particularly As, Sb, Te, W) anomalies
High fluid flux into structural trap sites in host rock sequences	Locked-up anticlinal or antiformal folds	Generally 30°–40° apical angles for assymmetrical folds with steep back limbs	Repetition of aeromagnetic signatures where there are suitable lithologies (absent in turbidite sequences)
	Thrust or oblique-slip duplexes	Thickening and duplication of host rock-sequences	Gravity gradients and complex aeromagnetic signatures
	Folded thrust sequences	Complex Kalgoorlie and Timmins-like structural geometries	Complex aeromagnetic signatures with anomalous closure within the regional aeromagnetic pattern
High fluid flux around margins of granite intrusions	Rigidity contrasts between minor intrusions and host rocks	Granite intrusions <1 km diameter within host sequences	Aeromagnetic and gravity gradients in district-scale surveys. Local geochemical anomalies
	Sheared margins of irregular granite intrusions	Changes in dip and/or strike of intrusion margins along curvilinear shear zones	Magnetic and gravity gradients in deposit-scale surveys. Discontinuous gold anomalies along granite intrusion contact
Fluid migration into stratigraphic trap sites	Strong rheology contrasts between units in rock sequences	Contrasts between competent and incompetent rock units	Largely undetectable via remote responses
	Reactive host rocks	Rock units with high Fe/(Fe + Mg) ratios or high C contents	High magnetic intensity pixels for Fe-rich rocks. IP or TEM anomalies for C-rich rock units
Fluid migration confined by caps or seals	Impermeable cap rocks	Low-permeability sedimentary sequences over fractured volcanic units at district to deposit scales: most common in Precambrian greenstone belts	Low aeromagnetic signatures of sedimentary rock sequences
	Structural seals	Thrust plates of impermeable rocks over more permeable units	Normally low aeromagnetic signatures of sedimentary units

lithostratigraphic proxies for Phanerozoic terranes, together with remnants of accreted Ocean Plate Stratigraphy (Maruyama et al., 1996; Safonova et al., 2009). Archean and Paleozoic convergent margins comprise more mafic-ultramafic sequences, resulting in the common terminology of greenstone belts, but arc-type volcanic rocks and turbidites are also present (Kawai et al., 2009). The high thermal flux in these settings is represented by voluminous granite batholiths and plutons, which dominate the preserved Archean and Paleoproterozoic convergent margin terranes. In a classic preserved sequence, these range from M- through I- to S- and A-type granites from the oceanic to continental margins of the convergent margins (L. Li et al., 2015; N. Li et al., 2015a, b), with hybrid intrusions adjacent to craton margins (Mair et al., 2011). Although metamorphic domains, inevitably of low-P Barrovian type, vary from sub-greenschist to upper amphibolite facies, greenschist-facies rocks dominate and granulite-facies are rare and blueschist-facies nearly totally absent in Archean terranes (Isozkai et al., 2010). The boundaries of the accreted terranes are marked by lithosphere-to crustal-scale faults or shear zones that extend along strike for hundreds to thousands of kilometres, and may be marked by lamprophyre and alkaline intrusions (Caroff et al., 2015). These are part of a classic D_0 to D_4 deformation sequence that involves initial rifting, thrusting, thrust reactivation, upright folding and oblique-slip as the stress regime evolves from extension through compression to transpression to orogenic collapse (Chetty and Bhaskar Rao, 2006).

A schematic diagram showing the major features of a convergent margin is presented in Fig. 9. In Archean and Paleoproterozoic terranes, mafic and ultramafic volcanic rocks dominate the greenstone belts which host the orogenic gold provinces.

From a geophysical viewpoint, these terranes are normally marked by quite subtle aeromagnetic and gravity signatures that are commonly dominated by contrasts with less- or more-magnetic and lower-gravity granite intrusions. In Fig. 10, the granite-greenstone terrane of the Yilgarn Block shows such a regional gravity pattern. The figure also clearly shows the craton-scale architecture of which the Yilgarn Block is part. It is only where there are Fe-rich lithostratigraphic units such as BIF units (Precambrian) or Fe-rich sills, at metamorphic-facies boundaries, or major boundaries between suspect terranes that there are strong magnetic contrasts within the supracrustal sequences. The major terrane-bounding faults or shear zones are normally clearly defined as lineaments on combined gravity-aeromagnetic images (Fig. 11). In terranes with superior pre-competitive geophysical data, that is available publicly from government sources, regional gravity surveys can better define the crustal architecture and highlight the deeper structures using multiscale edge analysis of potential field data or “worming” (Archibald et al., 1999). Orogenic gold districts commonly lie on gravity gradients (Bierlein et al., 2006a, b).

Where the convergent margin assemblages have undergone collisional tectonics or other tectonic interaction with craton or other lithosphere margins, the geological proxies are more complicated. There are commonly shelf-facies with carbonate units together with sandstone and shale sequences that overlie the more typical convergent margin assemblages (Fig. 9). There may be high metamorphic -grade basement juxtaposed against lower metamorphic-grade supracrustal sequences, commonly with complex fold-thrust interactions, and metamorphic core complexes developed in extreme cases (Zhang et al., 2018). The critical presence of metasomatized mantle lithosphere is indirectly detected by

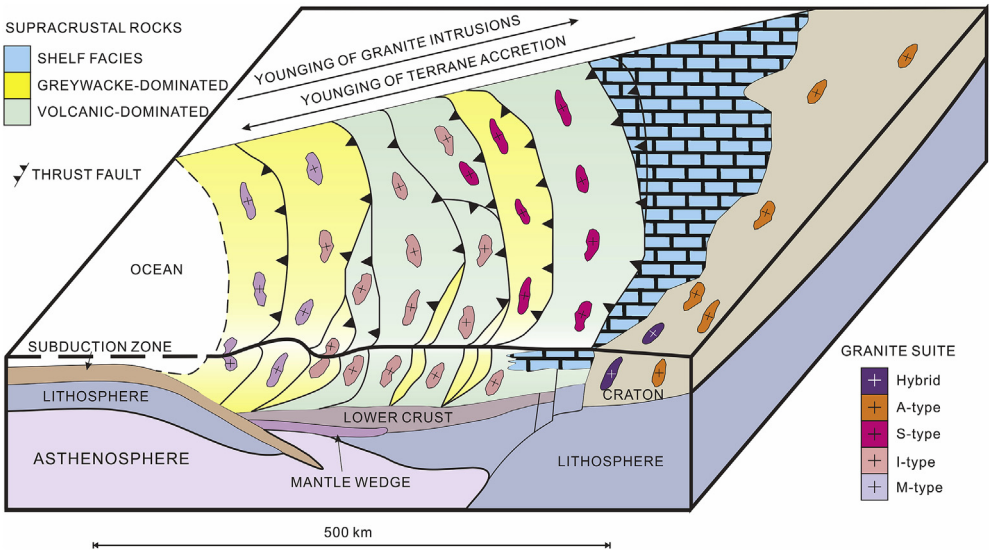

Fig. 9. Schematic block diagram indicating many of the critical features of a Phanerozoic convergent margin. Archean and Paleoproterozoic convergent margins are dominated by more mafic sequences in greenstone belts.

an anomalous abundance of hybrid (mixed mantle-crust derived) mafic to felsic intrusions (Mair et al., 2011), or directly detected by meta-somatized mantle xenoliths within alkaline intrusions (Saunders et al., 2018).

From a geophysical viewpoint, a combination of gravity, seismic and magneto-telluric data provide 2D to 3D representations of the complex structural geometry over the fragmented craton margin, but it is the aeromagnetic lineaments that normally best define the critical permeable fault zones up which sub-crustal auriferous fluids can migrate upwards into the crust as other geophysical data are commonly absent.

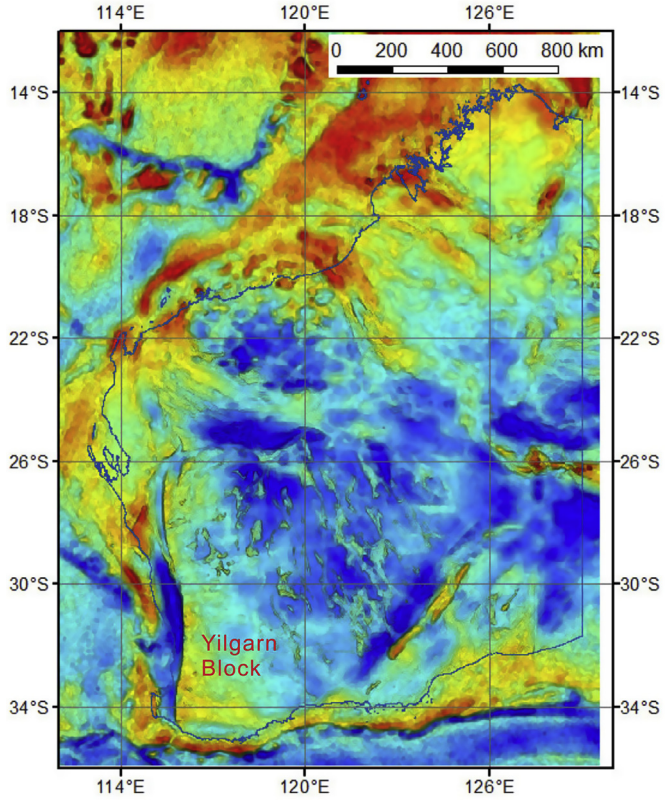

Fig. 10. Regional gravity image of Western Australia showing gross tectonic architecture with typical bouguer gravity signature of a granite (lower density)-greenstone belt (higher density) shown for the Yilgarn Block. Image courtesy of the Geological Survey and Resource Strategy, Department of Mines, Industry and Safety @ State of Western Australia 2019.

8. Architecture exploration factors

8.1. Province-scale parameters

At the province or terrane scale (Table 2), the architecture parameter of the mineral system model is closely linked to the geodynamics and fertility factors. The key architecture factor at this scale is provision of major permeable structures that extend to the Moho and can deliver high thermal and seismically-driven fluid flux from lithosphere to the crust (Fig. 8). As discussed above, for well-endowed gold provinces these are the first-order faults and shear zones that are marked by distinct aeromagnetic lineaments and commonly control the distribution of lamprophyres and related intrusions. Although seismic reflection sections are commonly used to portray the extent of these faults with depth, the faults are normally interpreted as shallowing thrusts (Owen et al., 1991: fig. 12), contrary to geological observations of these faults at varying depths along strike. It is the magneto-telluric sections (Dentith et al., 2013) that most clearly mark the vertical extent of these lineaments (Fig. 13). They conform to geological constraints that the aeromagnetic lineaments parallel or cross-cut metamorphic domain boundaries without deflection and all first-order structures from sub-greenschist- facies to upper-amphibolite-facies domains (<3 km to >15 km crustal depth) are steeply-dipping, as in the case of the Yilgarn Block of Western Australia.

Terranes with low-strain low-permeability sequences, indicated by preservation of primary structures and textures, with widely-spaced high-strain high-permeability shear zones provide greater opportunity for formation of world-class to giant mineral systems. This is because high fluid flux is focussed into a relatively small volume within the terrane, and is a major reason why Precambrian greenstone belts are so well endowed with orogenic gold (Groves et al., 2000). These first-order structures may also be marked by multi-element geochemical anomalism, as for example from geochemical surveys of laterites in the largely covered greenstone terranes of the Yilgarn Block in Western Australia (Butt and Zeegers, 1992).

More rapid uplift pene-contemporaneous with gold mineralization may also be an important regional factor. Giant gold districts, particularly Neoarchean examples, are commonly in districts where late conglomerate basins are juxtaposed against lower volcanic sequences (Abitibi Belt, Canada: Colvine et al., 1984; Norseman-Wiluna Belt, Western Australia: Tripp, 2014), with marked contrasts in magnetic intensity.

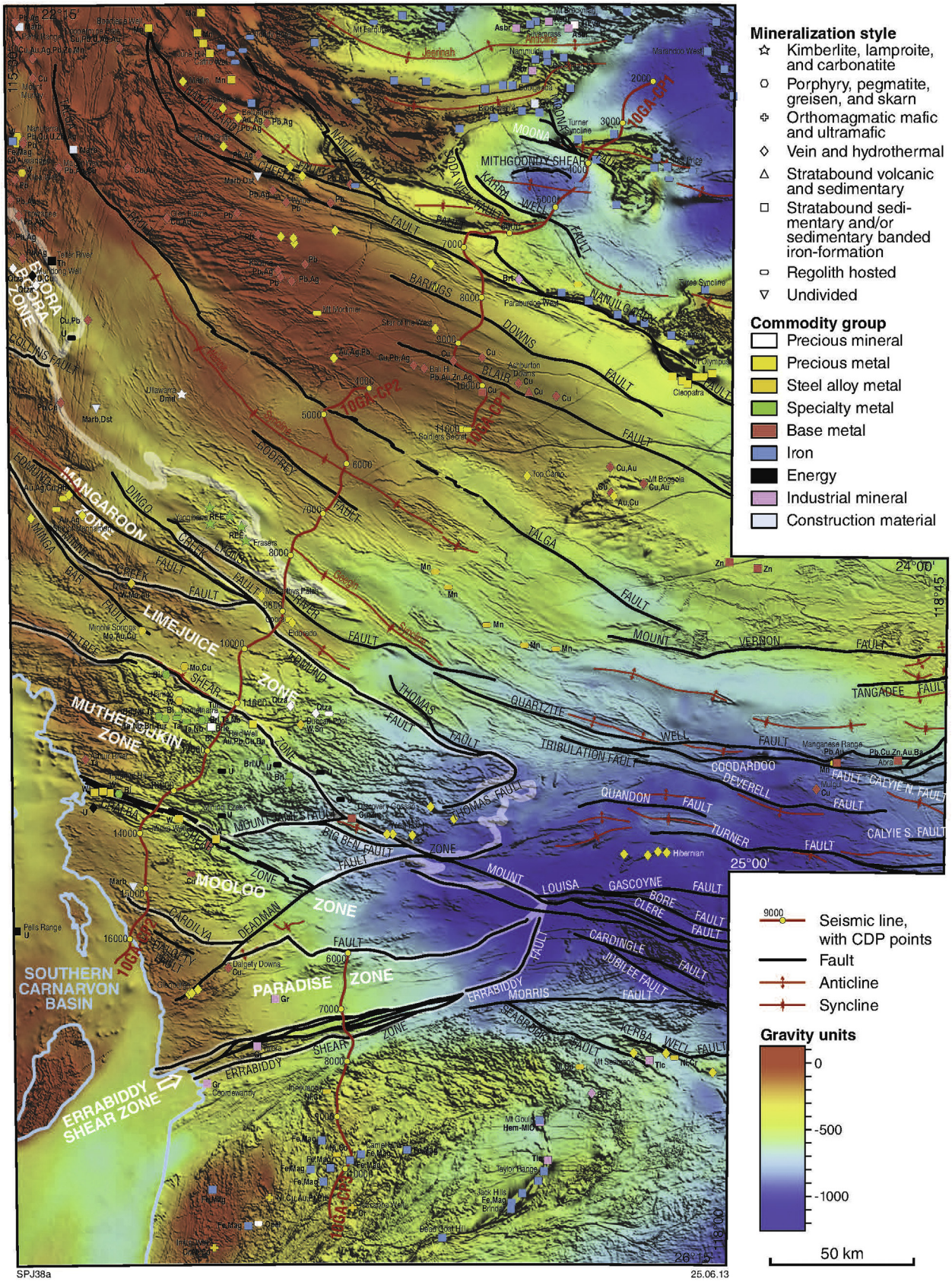

Fig. 11. Regional geophysical data for the western Capricorn Orogen with 2.5 km bouguer anomaly gravity data (colour) draped over 300–500 m line-spaced TMI aeromagnetic data (black and white). The location of the structural-metamorphic zone boundaries of the Gascoyne Province, major fault and mineral deposits is also shown. From Johnson et al. (2006).

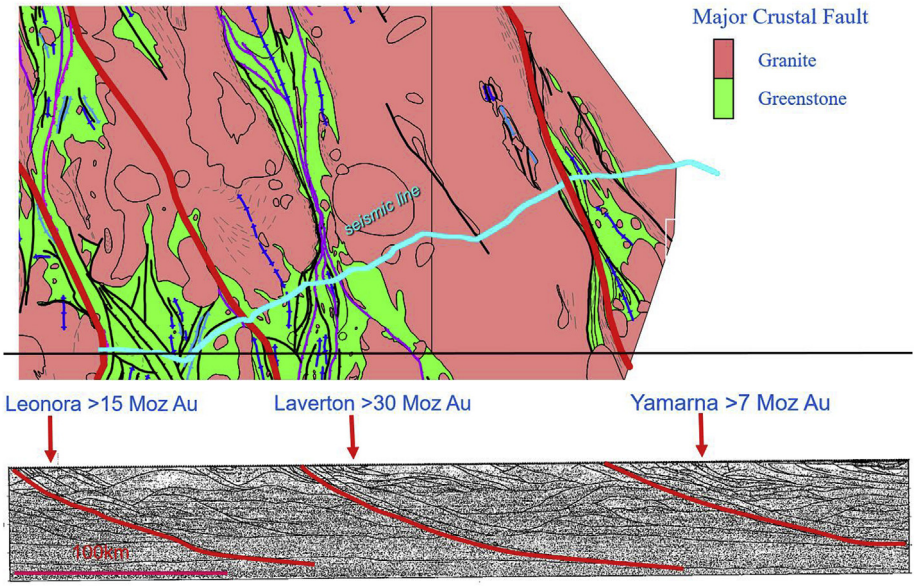

Fig. 12. Deep crust seismic reflection section across the greenstone belts and crustal-scale faults of the Yilgarn Block. Adapted from Owen et al. (1991): Geoscience Australia website.

These are interpreted to signify sites of anomalously rapid uplift rates along the first-order structures. Such rapid uplift lowers lithostatic pressures in interconnecting faults enhancing hydro-fracturing, inducing extreme pressure fluctuations, and leading to effective gold deposition through fluid un-mixing episodes (Groves et al., 1987). The same appears to hold for younger terranes in southern Alaska, where gold deposition is interpreted to have occurred on the retrograde limb of a clockwise Barrovian metamorphic P-T path as host rocks were rapidly uplifted (Goldfarb et al., 1986).

8.2. *District-scale fluid infiltration sites along first-order lineaments*

Those repetitive structural geometries that control the location of many orogenic gold deposits are described and discussed in considerable detail by Groves et al. (2018). They are briefly summarized below with reference to Table 3 and Fig. 14 and more extensive figures in Groves et al. (2018) where appropriate, with more emphasis here on the geological, geophysical and/or geochemical responses to critical geological parameters that have exploration significance.

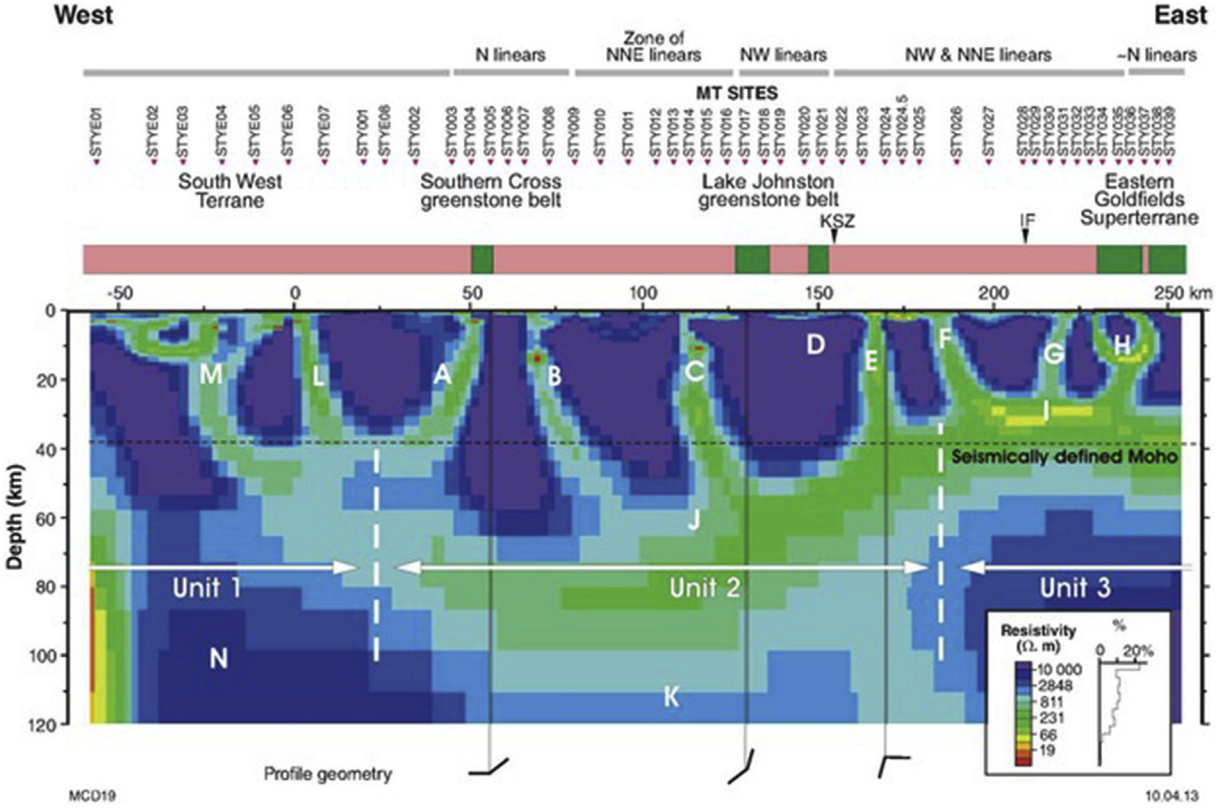

Fig. 13. Magnetotelluric section across the greenstone belts and crustal-scale faults of the Yilgarn Block. From Southern Cross Magnetotelluric Survey, 2011. Image courtesy of the Geological Survey and Resource Strategy, Department of Mines, Industry and Safety @ State of Western Australia 2019.

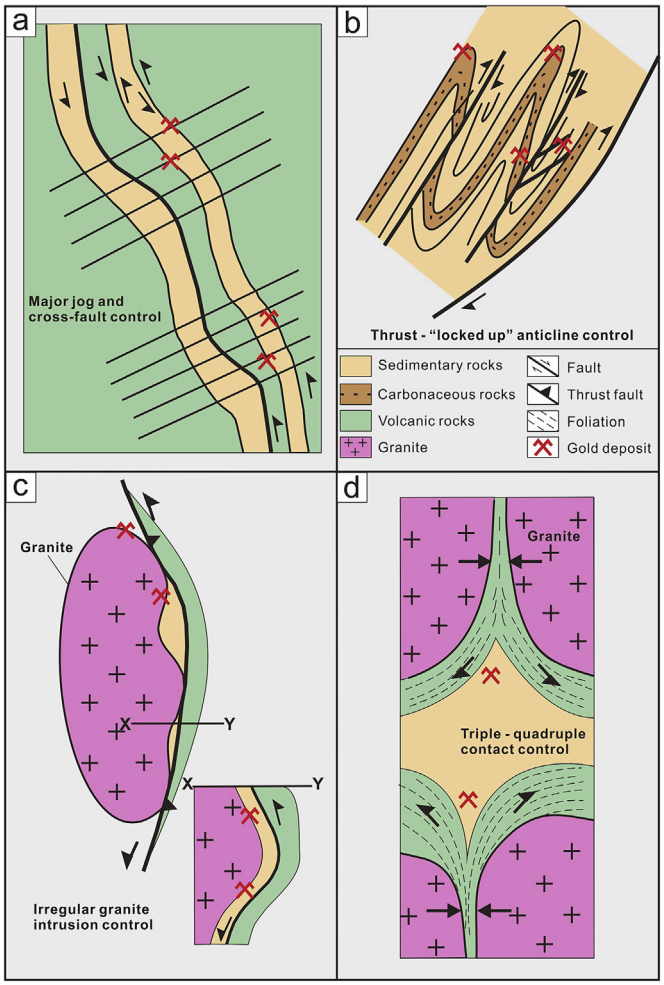

Fig. 14. Schematic diagrams showing repetitive structural architecture at fluid sinks or traps for orogenic gold systems: (a) major jogs on crustal-scale- and subsidiary faults/shear zones cut by corridors of accommodation faults; (b) "locked up" thrusted anticlinal folds; (c) irregular contacts on faulted margins of granite intrusions; (d) triple- and quadruple-point granite intrusion architecture.

Where crustal-to lithospheric-scale faults and shear zones are very linear with essentially the mean regional strike, they have no major damage zones and are consequently poorly gold-endowed. It is only along the curvilinear segments or jogs on these first-order structures that are 10°–25° off the mean trend (Groves et al., 2018: figs. 2 and 3), that the larger orogenic gold districts such as Kalgoorlie in Western Australia and Muruntau in Uzbekistan are sited (Weinberg et al., 2004). These districts are commonly spaced at intervals of ~30–35 km, broadly equivalent to depth to Moho, particularly where they host world-class deposits (Doutre, 2019, personal communication). It is also significant that some jogs, such as at Kalgoorlie (Weinberg et al., 2004) coincide with large-scale anticlinal structures, one of the most robust associations with orogenic gold, as discussed below.

At the district to deposit scale, orogenic gold deposits that are sited adjacent to these jogs may be hosted by a variety of faults or shear zones that pre-date gold mineralization: D_1 and D_2, less commonly D_3, structures as evident in most published D_1 to D_4 structural sequences (Vielreicher et al., 2016). However, subparallel arrays of obliquely cross-cutting faults that develop where there are flexures or jogs on the first-order faults, in many instances, provide the most important structural geometries in terms of predictive exploration (Groves et al., 2000, 2018: figs. 4–6). Worldwide, such accommodation fault arrays tend to be at ~70° to the local trend of the first-order structures and rock sequences, and are readily interpreted from arrays of aeromagnetic linear features oblique to the major aeromagnetic lineaments, with no mutual displacement. Groves et al. (2018) provide a variety of lines of evidence that these fault arrays control the location of gold deposits rather than post-date them, as suggested, for example at Kalgoorlie by Boulter et al. (1987), Mueller et al. (1988), Bateman and Hagemann (2004) and Weinberg et al. (2006). In many cases, the gold deposits are located in pre-gold structures between two of these accommodation faults that have the same sense of motion. Examples from Western Australia include Mt Charlotte and the Golden Mile at Kalgoorlie and Kundana (Groves et al., 2018: figs. 4 and 5) and from China include Huangjindong (Zhang et al., 2018, 2019a).

Insights into the structural mechanisms that lead to such controls can be gained from research in non-mineralized terranes in California (Nicholson et al., 1986; Jackson and Molnar, 1990) and in Alaska (Page et al., 1995). These studies describe rotation and torsional strain within the blocks between pairs of kinematically-compatible faults with the same sense of movement (Groves et al., 2018: fig. 7). This rotation of fault blocks and their internal pre-existing structures, due to the opposite fault motion on either side of the bounding paired faults, causes reactivation of, and inhomogeneous strain within, those internal structures. This leads to focussed fluid flux into dilation and other damage zones along suitably-aligned pre-existing structures and deposition of high-grade gold ores within those structures and more disseminated mineralization and alteration zones adjacent to them. There may be distinctive multi-element geochemical anomalies (Au, As, Sb, Te, and W) and distinct changes in the hyperspectral signature of alteration micas (Wang et al., 2017) at these intersection points.

8.3. District- to deposit-scale fluid infiltration sites at antiformal traps

Many authors have designated anticlines, or antiforms, the most robust fluid traps for orogenic gold deposits at the district to deposit scale (Goldfarb et al., 2005). Cox et al. (1991) showed that turbidite-hosted deposits now termed orogenic gold deposits formed when folds became 'locked up', with faulting and fracturing replacing flexural folding as the predominant deformation mechanism. The locked-up folds tend to be asymmetrical folds with apical angles of approximately 30° and overturned back limbs, modified by thrusts and fracture arrays that promote focussed fluid flux and resultant gold deposition (Leader et al., 2010). As shown by Groves et al. (2018: fig. 8b–h), these fold characteristics are common to a wide range of orogenic gold deposits of different age and host sequences globally.

It is evident that district-to deposit-scale anticlinal or antiformal folds with ~30° apical angles, commonly with associated thrusts, are a predictable and repetitive characteristic of many orogenic gold deposits of all ages. They have highly variable geophysical signatures (Table 3) dependant on their host sequences. Related thrust or oblique-slip duplexes may be detected via complex aeromagnetic signatures and gravity gradients. The two giant Archean orogenic gold deposits at the Golden Mile, Kalgoorlie and Timmins, Abitibi Belt, formed within complex, duplicated (Golden Mile) antiformal structures due to folding of pre-existing thrust faults (Groves et al., 2000: fig. 5).

8.4. District- to deposit-scale fluid infiltration sites around granite intrusions

The important exploration aspects of the mineral system architecture parameter discussed above deal exclusively with structures confined to the convergent margin volcano-sedimentary sequences in orogenic gold provinces. Granite intrusions are a common component in orogenic gold provinces as a reflection of high thermal gradients related to subduction-related orogenesis (Goldfarb et al., 2005). They may be pre-gold, relatively rare syn-gold, or post-gold intrusions, with no consistent spatial or genetic relationship to the orogenic gold deposits (Goldfarb and Groves, 2015). However, in some gold provinces, particularly in Archean and Paleoproterozoic granite-dominated terranes, pre-to syn-gold intrusions

may play an important structural role for the location of both gold districts or camps and individual gold deposits. This is discussed below, with emphasis on the district scale.

As shown somewhat schematically in Fig. 14c and d, individual rigid granitic intrusions, whether having sheared or complex intrusive contacts with volcano-sedimentary sequences, can cause significant variations in the orientation of local principal maximum stress relative to the externally-imposed regional stress. These may cause anomalously-low minimum stress zones on a deposit scale related to variations in the geometry of the immediate contact zones (Granny Smith in Western Australia: Ojala et al., 1993) or on a district scale related to complexities in the regional geometry of the intrusion contact (Coolgardie Goldfield, Western Australia: Knight et al., 1993). These low minimum-stress zones can localise fluid flux and become the loci of gold mineralization (Ridley, 1993).

Complexities in structural geometry compound where two or more adjacent rigid granite intrusions impinge on more ductile volcano-sedimentary sequences, as in the Barberton Goldfield of South Africa (Groves et al., 2018: fig. 10). In these settings, significant gold deposits are normally located in thrust or oblique-slip duplexes within V-shaped neck zones that represent strain gradients between the compressional high-strain zone of thinning between the adjacent granite intrusions and the low strain supracrustal sequences distal to the intrusions. Fluid flux is directed to these zones of heterogeneous stress with gold deposits deposited in structural sites within them.

More complex structural geometries are developed at triple-point junctions between three granitic bodies that impinge on the volcano-sedimentary sequences. Gold deposits are again located along strain gradients in heterogeneous stress zones within inverted V-shaped or cuspate volcano-sedimentary segments of belts. Groves et al. (2018: fig. 11) show an example from the Southern Cross Greenstone Belt in Western Australia, but there are world-wide examples including Red Lake, Eleonore, and Musselwhite in Canada, the deposits of the Quadrilatero Ferrifero in Brazil, and those in the Fennoscandian Shield.

From an exploration viewpoint, these triple- and even quadruple-point junctions are evident on available aeromagnetic images (Fig. 15) and are commonly on gravity gradients due to magnetic susceptibility and density contrasts between granite intrusions and supracrustal sequences, particularly in Precambrian greenstone belts.

As discussed in more detail by Groves et al. (2018), such triple point junctions have also been identified as potential sites for gold mineralization on a geodynamic scale in recent studies such as those in the North China Craton. For example, Li and Santosh (2017) identified that most of the major gold deposits, including the giant Jiaodong gold province,

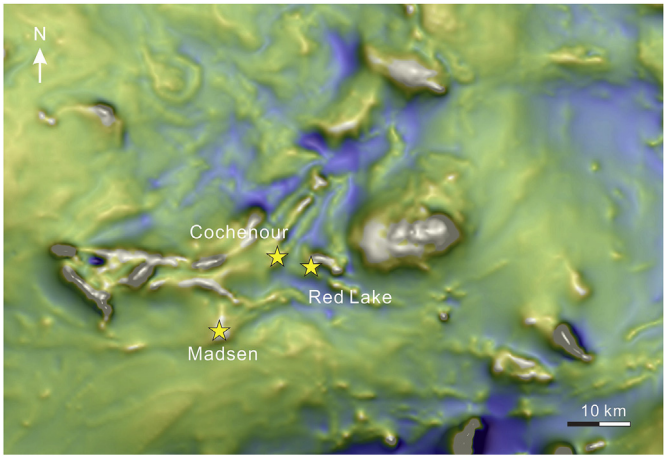

Fig. 15. Aeromagnetic image showing gold deposits in the Red Lake gold district, Superior Province of Canada, located at a triple-point/quadruple-point junction of granitic batholiths. Image courtesy of Francis Macdonald of Kenorland Minerals.

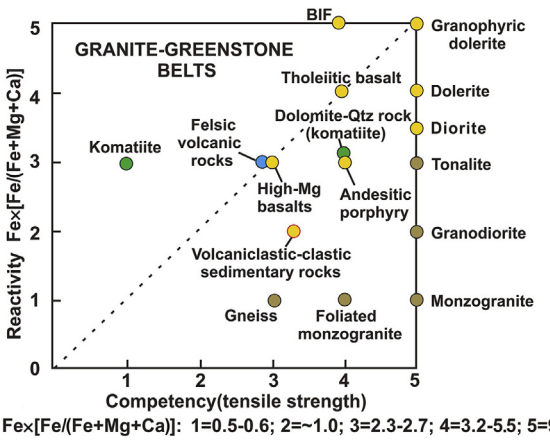

Fig. 16. Reactivity vs. rheology (competency) plot for potential host rocks to orogenic gold deposits in granite-greenstone belts. X and Y axes are empirically numbered 1–5 due to difficulty in obtaining representative quantitative values. Rocks in right-hand upper corner are preferred host rocks due to their Fe-rich nature and susceptibility to brittle failure.

associated with the Mesozoic giant metallogenic provinces in the North China Craton are located along the zones of amalgamation of two or three paleo micro-blocks, making such zones important targets for terrane-scale exploration.

8.5. *Deposit-scale stratigraphic trap and cap sites*

Structure clearly plays the major role in focussing large volumes of auriferous fluid into small volumes of rock and forming high-grade vein-type gold deposits. However, the nature of the rock sequences plays the major role in the formation of bulk-tonnage lower-grade disseminated orebodies suitable for modern mining. As noted in Table 3, both rheology and geochemistry of the potential host rocks play a major role. There must be a favourable fluid pathway to the rheologically or geochemically prospective rocks (Hronsky, 2019).

Rheological contrasts between rock types in the potential host sequences play an important role in selective failure of more competent units to provide specific permeability channels for fluid migration and fluid-rock reaction. Decreases from supralithostatic to hydrostatic pressure related to such hydraulic fracturing (Sibson, 1992; Cox et al., 2001) leads to fluid immiscibility and direct gold precipitation (Loucks and Mavrogenes, 1999). Fluid reaction with Fe-rich rocks such as BIFs, basalts, dolerites and diorites, that have high magnetic susceptibility, also leads to gold deposition via sulfidation reactions (Phillips et al., 1984; Bohlke, 1988) and other wallrock reactions (Evans et al., 2006). Carbonaceous material may play a role in fluid reduction and gold deposition in carbon-rich sedimentary host rocks (Wilson et al., 2013), which may be defined by IP or TEM anomalism. A schematic plot of rheology vs reactivity in Fig. 16 demonstrates how potential host rocks for orogenic gold deposits might be assessed with basic knowledge of litho-stratigraphic successions and igneous intrusions.

It is also important that the auriferous fluid is impounded within the depositional site and not be able to readily exit the hydrothermal system. Such caps are normally provided by rheology contrasts between the gold system and overlying units. For Precambrian deposits, the cap is commonly provided by more ductile sedimentary units that overly more competent volcanic-dominated sequences (Groves et al., 2000), but the cap may be more subtle in Phanerozoic deposits in dominantly sedimentary sequences. There will inevitably be some fluid outflow potentially defined by anomalous but metal-poor carbonate-mica alteration zones that could appear as magnetic lows if destruction of Fe-rich minerals was involved in alteration.

A more detailed discussion of the processes that control the location and geometry of the mineralized envelope and the gold ore shoots within

it for the orogenic gold system is given by Hronsky (2019) and is not repeated here. They are more important at the drill stage than the target generation stage.

9. Preservation exploration factors

As noted above, orogenic gold systems are anomalous in that they can form at deep crustal levels and may individually extend to > 2 km down dip or plunge, explaining their distribution throughout most of geologic time (Goldfarb et al., 2001). Whether they are exposed at or close to the surface depends on exhumation and erosion. The degree of exhumation for any terrane can be accurately deduced from thermo-chronological studies (Zhang et al., 2019b), However, from a more practical viewpoint, the geologically deduced level of erosion of known deposits can be a good exploration guide. As discussed above, the structural and alteration characteristics, combined with their metal associations, can be used to group them into epizonal, mesozonal and hypozonal groups (Gebre-Mariam et al., 1995). A terrane having mostly epizonal Au–Sb deposits, for example, clearly has the potential to host deeper mesozonal deposits, either beneath epizonal deposits, or elsewhere in the terrane. In contrast, a terrane dominated by hypozonal deposits has more limited future potential, although orebodies in the giant Kolar hypozonal deposit did extend for more than 2 km depth below surface (Radhakrishna and Curtis, 1999; Sarma et al., 2011).

10. Conclusions

Any mineral system has to be anchored by the fundamental Earth processes incorporated in geodynamics, fertility, architecture and preservation. For orogenic gold systems, fertility is inexorably linked to subduction, so that geodynamics and fertility parameters are both related to convergent margin tectonics. Fertile gold fluids are either directly related to devolatilization of the subducted slab and overlying sediment wedge, or indirectly related to reactivated mantle lithosphere previously metasomatized by such fertile subduction-related fluids. The first-order components of the orogenic gold system architecture are lithosphere-to-crust-scale faults or shear zones capable of delivering a focussed flux of auriferous fluid to the crust during seismic activity, preferably to crustal levels equivalent to the ductile-brittle transition. Within the crust, fluid is further focussed into spaced damage zones, normally jogs or flexures in the first-order fluid channels via injection-driven swarm seismology. Here, the fluid migrates along pressure gradients to lower-order, interconnected structures with repetitive architectures, related to critical controls such as fault arrays, locked-up anticlinal hinges, or anomalous configurations of igneous intrusions. Conjunctions of these parameters produce the world-class to giant deposits. At these structural sites, depositional traps and caps connected to favourable fluid pathways are controlled by rheology and geochemical contrasts between rock units in the host rock sequences. The deposits normally survive exhumation and erosion because of their deep crustal formation and extensive vertical extent, and, in the case of Precambrian deposits, the formation of thick buoyant lithosphere soon after gold mineralization. It is only the period from the Mesoproterozoic to early Neoproterozoic that is largely devoid or orogenic gold deposits.

From an exploration viewpoint, the orogenic gold system model provides a hierarchical framework for target generation. Ancient convergent margins can first be recognized from a number of geological and geophysical proxies outlined above. Strike-extensive faults that extend to the Moho can be best identified as aeromagnetic lineaments in poorly-explored terranes, or as magneto-telluric anomalous zones in more mature terranes. They may also have deeply-sourced intrusions, such as lamprophyre dykes along them. The wide range of structural and stratigraphic traps related to interconnected lower-order structures can be recognized by repetitive structural geometries derived from both geological and geophysical data. Gravity "worms" and gradients may be particularly diagnostic. Locations within these geometries that comprise rock sequences with the required rheological and geochemical characteristics to represent traps and caps can then be identified as specific exploration targets. These are likely to have a multi-element geochemical footprint if a significant deposit exists at the target site.

Declaration of competing interest

The authors declare that they have no known competing financial interest or personal relationships that could have appeared to influence the work reported in this paper.

Acknowledgements

We thank Dr. V.O. Samuel, Assocaite Editor for handling our paper and Dr. Cheng-Xue Yang for her helpful and constructive review. We are indebted to many colleagues over many years who have contributed to our knowledge of gold mineralization and associated tectonic environments and processes. We are particularly indebted to Rich Goldfarb, formerly of the USGS and now a consultant, for his invaluable contributions. DIG is indebted to Jun Deng, Qingfei Wang and Liqiang Yang for the opportunity to interact with them and their research projects at CUGB. Simon Johnson is thanked for suppling a high-quality image of Fig. 11. The research was partly funded by the National Natural Science Foundation of China (Grant Nos. 41230311, 41572069, 41702070), the National Key Research and Development Project of China (2016YFC0600307), the National Key Research Program of China (Grant Nos. 2016YFC0600107-4 and 2016YFC0600307), the MOST Special Fund from the State Key Laboratory of Geological Processes and Mineral Resources, China University of Geosciences (Grant No. MSFGPMR201804) and the 111 Project of the Ministry of Science and Technology, China (Grant No. BP0719021).

References

Archibald, N., Gow, P., Boschetti, F., 1999. Multiscale edge analysis of potential field data. Explor. Geophys. 32, 48–55.
Baker, T., 2002. Emplacement depth and CO_2–rich fluid inclusions in intrusion-related gold deposits. Econ. Geol. 97, 1109–1115.
Bateman, R.J., Hagemann, S.G., 2004. Gold mineralisation throughout about 45 Ma of Archaean orogenesis: protracted flux of gold in the golden mile, Yilgarn craton, western Australia. Miner. Depos. 39, 536–559.
Begg, G.C., Griffin, W.L., Natapov, L.M., O'Reilly, S.Y., Grand, S.P., O'Neill, C.J., Hronsky, J.M.A., Poudjom Djomani, Y., Swain, C.J., Deen, T., Bowden, P., 2009. The lithospheric architecture of Africa: seismic tomography, mantle petrology and tectonic evolution. Geosphere 5, 23–50.
Bierlein, F.P., Groves, D.I., Goldfarb, R.J., Dube, B., 2006. Lithospheric controls on the formation of giant orogenic gold deposits. Miner. Depos. 40, 874–886.
Bierlein, F.P., Murphy, F.C., Weinberg, R., Lees, T., 2006. Distribution of orogenic gold deposits in relation to fault zones and gravity gradients: targeting tools applied to the Eastern Goldfields, Yilgarn Craton, Western Australia. Miner. Depos. 41, 107–126.
Bierlein, F.P., Pisarevsky, S., 2008. Plume-related oceanic plateaus as a potential source of gold mineralization. Econ. Geol. 103, 425–430.
Bloem, E.J.M., Dalstra, H.J., Groves, D.I., Ridley, J.R., 1994. Metamorphic and structural setting of Archaean amphibolite-hosted gold deposits near Southern Cross, Southern Cross Province, Yilgarn Block, Western Australia. Ore Geol. Rev. 9, 183–208.
Böhlke, J.K., 1988. Carbonate-sulphide equilibria and "stratabound" disseminated epigenetic gold mineralization: a proposal based on Alleghany, California, USA. Appl. Geochem. 3, 499–516.
Bouchot, V., Ledru, P., Lerouge, C., Lescuyer, J.-L., Milesi, J.-P., 2005. Late Variscan mineralizing systems related to orogenic processes: the French Massif Central. Ore Geol. Rev. 27, 169–197.
Boulter, C.A., Fotios, M.G., Phillips, G.N., 1987. The Golden Mile, Kalgoorlie: a giant gold deposit localized in ductile shear zones by structurally induced infiltration of auriferous metamorphic fluids. Econ. Geol. 82, 1661–1678.
Boyle, R.W., 1979. The geochemistry of gold and its deposits. Geol. Surv. Can. Bull. 280, 584.
Breeding, C.M., Ague, J.J., 2002. Slab-derived fluids and quartz-vein formation in an accretionary prism, Otago Schist, New Zealand. Geology 30, 499–502.
Browning, P., Groves, D.I., Blockley, J.G., Rosman, K.J.R., 1987. Lead isotope constraints on the age and source of gold mineralization in the Archean Yilgarn Block, Western Australia. Econ. Geol. 82, 971–986.
Bureau, Hln, Keppler, H., 1999. Complete miscibility between silicate melts and hydrous fluids in the upper mantle: experimental evidence and geochemical implications. Earth Planet. Sci. Lett. 165, 187–196.

Burnard, P.G., Polya, D.A., 2004. Importance of mantle derived fluids during granite associated hydrothermal circulation: He and Ar isotopes of ore minerals from Panasqueira. Geochem. Cosmochim. Acta 68, 1607–1615.
Butt, C.R.M., Zeegers, H., 1992. Regolith exploration geochemistry in tropical and subtropical terrains. In: Handbook of Exploration Geochemistry, vol 4. Elsevier, Amsterdam, p. 607.
Caroff, M., Labry, C., Le Gall, B., Authemayou, C., Guillong, M., 2015. Petrogenesis of late-Variscan high K alkali-calcic granitoids and calc-alkalic lamprophyres: the Aber/IIdut/North-Ouessant complex, Armorican Massif, France. Lithos 238, 140–155.
Cawood, P.A., Kröner, A., Collins, W.J., Kusky, T.M., Mooney, W.D., Windley, B.F., 2009. Accretionary orogens through Earth history. Geol. Soc. Lond. Spec. Publ. 318, 1–36.
Chen, Y.J., Pirajno, F., Qi, J.P., 2008. The Shanggong gold deposit, Eastern Qinling Orogen, China— isotope geochemistry and implication for ore genesis. J. Asian Earth Sci. 33, 252–266.
Chetty, T.R.K., Bhaskar Rao, Y.J., 2006. The Cauery Shear Zone, Southern Granulite Terrain, India: a crust-scale flower structure. Gondwana Res. 10, 77–85.
Cline, J.S., Hofstra, A.H., Muntean, J.L., Tosdal, R.M., Hickey, K.A., 2005. Carlin-type gold deposits in Nevada: critical geologic characteristics and viable models. In: Economic Geology 100th Anniversary, pp. 451–484.
Colvine, A.C., Andrews, A.J., Cherry, M.E., Durocher, M.E., Fyon, J.A., Lavigne, M.J., Macdonald, A.J., Marmont, S., Poulsen, K.H., Springer, J.S., Troop, D.G., 1984. An integrated model for the origin of Archean lode-gold deposits. In: Ontario Geological Survey Open-File Report, 5524, p. 98.
Colvine, A.C., Fyon, J.A., Heather, K.B., Marmont, S., Smith, P.M., Troop, D.G., 1988. Archean lode gold deposits in Ontario. Ont. Geol. Surv. Misc. Pap. 139, 136.
Cox, S.F., 2016. Injection-driven swarm seismicity and permeability enhancement: implications for the dynamics of hydrothermal ore systems in high fluid-flux, over-pressured faulting regimes—an invited paper. Econ. Geol. 111, 559–588.
Cox, S.F., Etheridge, M.A., Cas, R.A.F., Clifford, B.A., 1991. Deformational style of the Castlemaine area, Bendigo-Ballarat Zone–implications for evolution of the crustal structure across southeast Australia. Aust. J. Earth Sci. 38, 151–170.
Cox, S.F., Knackstedt, M.A., Braun, J., 2001. Principles of structural control on permeability and fluid flow in hydrothermal systems. Econ. Geol. Rev. 14, 1–24.
Davies, R.S., Groves, D.I., Trench, A., Dentith, M., Sykes, J.P., 2019. Appraisal of the USGS three-part assessment through evaluation of an orogenic gold exploration project in the sandstone greenstone belt, Yilgarn craton, western Australia. Miner. Depos. https://doi.org/10.1007/s00126-019-00916-1.
Davies, R.S., Groves, D.I., Trench, A., Sykes, J.P., Standing, J.G., 2018. Entering an immature exploration search space: assessment of the potential orogenic gold endowment of the Sandstone Greenstone Belt, Yilgarn Craton, by application of Zipf's law and comparison with the adjacent Agnew Goldfield. Ore Geol. Rev. 94, 326–350.
de Boorder, H., 2012. Spatial and temporal distribution of the orogenic gold deposits in the Late Palaeozoic Variscides and Southern Tianshan—how orogenic are they? Ore Geol. Rev. 46, 1–31.
Deng, J., Wang, C.M., Bagas, L., Santosh, M., Yao, E.Y., 2018. Crustal architecture and metallogenesis in the south-eastern North China Craton. Earth Sci. Rev. 182, 251–272.
Deng, J., Wang, Q.F., 2016. Gold mineralization in China: metallogenic provinces, deposit types and tectonic framework. Gondwana Res. 36, 219–274.
Deng, J., Wang, Q.F., Santosh, M., Liu, X., Liang, Y., Yang, L.Q., Zhao, R., Yang, L., 2019. Remobilization of metasomatized mantle lithosphere: a new model for the Jiaodong gold province, eastern China. Miner. Depos. https://doi.org/10.1007/s00126-019-00925-0.
Deng, J., Yang, L.Q., Li, R.H., Groves, D.I., Santosh, M., Wang, Z.L., Sai, X.S., Wang, S.R., 2019. Regional structural controls on the distribution of giant to world-class gold deposits in the Jiaodong gold province, China. Geol. J. 54, 378–391.
Deng, J., Yang, L.Q., Sun, Z.S., Wang, J.P., Wang, Q.F., Xin, H.B., Li, X.J., 2003. A metallogenic model of gold deposits of the Jiaodong granite-greenstone Belt. Acta Geol. Sin. 77, 537–546.
Dentith, M.D., Aitkin, A., Evans, S., Joly, A., 2013. Regional targeting for gold and nickel deposits using crustal electrical conductivity variations determined using the magnetotelluric method. Austr. Soc. Explor. Geophys. Extend. Abstr. 124, 1–4.
Dong, Y.P., Santosh, M., 2016. Tectonic architecture and multiple orogeny of the Qinling orogenic belt, Central China. Gondwana Res. 29, 1–40.
Evans, K.A., Phillips, G.N., Powell, R., 2006. Rock-buffering of auriferous fluids in altered rocks associated with the Golden Mile-style mineralization, Kalgoorlie gold field, Western Australia. Econ. Geol. 101, 805–817.
Finlay, A.J., Selby, D., Osborne, M.J., Finucane, D., 2010. Fault-charged mantle-fluid contamination of United Kingdom North Sea oils: insights from Re-Os isotopes. Geology 38, 979–982.
Fyfe, W.S., Price, N.J., Thompson, A.B., 1978. Fluids in the Earth's crust. Elsevier, Amsterdam, p. 383 pp.
Gao, L., Wang, Q.F., Deng, J., Zhang, S.H., Yang, Z.Y., 2018. Relationship between orogenic gold mineralization and crustal shearing along Ailaoshan-Red River Belt, southeastern Tibetan Plateau: new constraint from paleomagnetism. Geochem. Geophys. Geosyst. 19, 2225–2242.
Gebre-Mariam, M., Hagemann, S.G., Groves, D.I., 1995. A classification scheme for epigenetic Archaean lode-gold deposits. Miner. Depos. 30, 408–410.
Goldfarb, R.J., Baker, T., Dubé, B., Groves, D.I., Hart, C.J.R., Gosselin, P., 2005. Distribution, character, and genesis of gold deposits in metamorphic terranes. In: Economic Geology 100th Anniversary, pp. 407–450.
Goldfarb, R.J., Groves, D.I., 2015. Orogenic gold: common vs evolving fluid and metal sources through time. Lithos 223, 2–26.
Goldfarb, R.J., Groves, D.I., Gardoll, S., 2001. Orogenic gold and geologic time; a global synthesis. Ore Geol. Rev. 18, 1–75.
Goldfarb, R.J., Hart, C.J.R., Davis, G., Groves, D.I., 2007. East Asian gold—deciphering the anomaly of Phanerozoic gold in Precambrian cratons. Econ. Geol. 102, 341–346.
Goldfarb, R.J., Leach, D.L., Miller, M.L., Pickthorn, W.J., 1986. Geology, Metamorphic Setting, and Genetic Constraints of Epigenetic Lode-Gold Mineralization within the Cretaceous Valdez Group, South-Central Alaska, vol 32. Geological Association of Canada Special Paper, pp. 87–105.
Goldfarb, R.J., Leach, D.L., Pickthorn, W.J., Paterson, C.J., 1988. Origin of lode–gold deposits of the Juneau gold deposit, southeast Alaska. Geology 16, 440–443.
Goldfarb, R.J., Santosh, M., 2014. The dilemma of the Jiaodong gold deposits: are they unique? Geosci. Front. 5, 139–153.
Goldfarb, R.J., Taylor, R.D., Collins, G.S., Goryachev, N.A., Orlandini, O.F., 2014. Phanerozoic continental growth and gold metallogeny of Asia. Gondwana Res. 25, 48–102.
Goldfarb, R.J., Qiu, K.F., Deng, J., Chen, Y.J., Yang, L.Q., 2019. Orogenic Gold Deposits of China. In: Chang, Z.S., Goldfarb, R.J. (Eds.), Mineral Deposits of China. Society of Economic Geologists Special Publication, 22, p. 263–324. https://doi.org/10.5382/SP22.08.
Griffin, W.L., Begg, G.C., O'Reilly, S.Y., 2013. Continental root control on the genesis of magmatic ore deposits. Nat. Geosci. 6, 905–910.
Griffin, W.L., Zhang, A., O'Reilly, S.Y., 1998. Phanerozoic evolution of the lithosphere beneath the Sino-Korean craton. In: Fowler, M.F.J. (Ed.), Mantle Dynamics and Plate Interactions in East Asia, vol 27. American Geophysical Union Geodynamics Series, pp. 107–126.
Groves, D.I., 1993. The crustal continuum model for late-Archaean lode gold deposits of the Yilgarn block, Western Australia. Miner. Depos. 28, 366–374.
Groves, D.I., Condie, K.C., Goldfarb, R.J., Hronsky, J.M.A., Vielreicher, R.M., 2005a. Secular changes in global tectonic processes and their influence on the temporal distribution of gold-bearing mineral deposits. In: Economic Geology 100th Anniversary, pp. 203–224.
Groves, D.I., Goldfarb, R.J., Gebre-Mariam, M., Hagemann, S.G., Robert, F., 1998. Orogenic gold deposits–a proposed classification in the context of their crustal distribution and relationship to other gold deposit types. Ore Geol. Rev. 13, 7–27.
Groves, D.I., Goldfarb, R.J., Knox-Robinson, C.M., Ojala, J., Gardoll, S., Yun, G., Holyland, P., 2000. Late-kinematic timing of orogenic gold deposits and its significance for computer-based exploration techniques with emphasis on the Yilgarn block, Western Australia. Ore Geol. Rev. 17, 1–38.
Groves, D.I., Goldfarb, R.J., Robert, F., Hart, C.J.R., 2003. Gold deposits in metamorphic belts: overview of current understanding, outstanding problems, future research, and exploration significance. Econ. Geol. 98, 1–29.
Groves, D.I., Goldfarb, R.J., Santosh, M., 2016. The conjunction of factors that lead to formation of giant gold provinces and deposits in non-arc settings. Geoscience Frontiers 7 (3), 303–314.
Groves, D.I., Phillips, G.N., Ho, S.E., Houstoun, S.M., Standing, C.A., 1987. Craton-scale distribution of Archean greenstone gold deposits—predictive capacity of the metamorphic model. Econ. Geol. 82, 2045–2058.
Groves, D.I., Santosh, M., 2015. Province-scale commonalities of some world-class gold deposits: implications for mineral exploration. Geosci. Front. 6, 389–399.
Groves, D.I., Santosh, M., 2016. The giant Jiaodong gold province: the key to a unified model for orogenic gold deposits? Geosci. Front. 7, 409–418.
Groves, D.I., Santosh, M., Deng, J., Wang, Q.F., Yang, L.Q., Zhang, L., 2019. A holistic model for the origin of orogenic gold deposits and its implications for exploration. Miner. Depos. https://doi.org/10.1007/s00126-019-00877-5.
Groves, D.I., Santosh, M., Goldfarb, R.J., Zhang, L., 2018. Structural geometry of orogenic gold deposits: implications for exploration of world-class and giant deposits. Geosci. Front. 9, 1163–1177.
Groves, D.I., Vielreicher, R.M., Goldfarb, R.J., Condie, K.C., 2005b. Controls on the heterogeneous distribution of mineral deposits through time. In: McDonald, I., Boyce, A.J., Butler, I.B., Herrington, R.J., Polya, D.A. (Eds.), Mineral Deposits and Earth Evolution, vol 248. Geological Society of London Special Publication, pp. 71–102.
Hagemann, S.G., Lisitsin, V.A., Huston, D.L., 2016. Mineral system analysis: quo vadis. Ore Geol. Rev. 76, 504–522.
Hedenquist, J.W., Lowenstern, J.R., 1994. The role of magmas in the formation of hydrothermal ore deposits. Nature 370, 519–527.
Hronsky, J.M.A., 2011. Self-organized critical systems and ore formation: the key to spatial targeting? Soc. Econ. Geol. Newslett. 84, 14–16.
Hronsky, J.A., 2019. Deposit-scale structural controls on orogenic gold deposits: an integrated, physical process based hypothesis and practical targeting implications. Miner. Depos. https://doi.org/10.1007/s00126-019-00918-z.
Hronsky, J.M.A., Groves, D.I., Loucks, R.R., Begg, G.C., 2012. A unified model for gold mineralisation in accretionary orogens and implications for regional-scale exploration targeting methods. Miner. Depos. 47, 339–358.
Hronsky, J., Groves, D., 2008. Science of targeting: Definition, strategies, targeting and performance measurement. Australian Journal of Earth Sciences 55, 3–12.
Huston, D.L., Mernagh, T.P., Hagemann, S.G., Doublier, M.P., Fiorentini, M., Champion, D.C., Jaques, A.L., Czarnota, K., Cayley, R., Bastrakov, R.S., 2016. Tectono-metallogenic systems—The place of mineral systems within tectonic evolution, with an emphasis on Australian examples. Ore Geol. Rev. 76, 168–210.
Hyndman, R.D., McCrory, P.A., Wech, A., Kao, H., Ague, J., 2015. Cascadia subducting plate fluids channeled to forearc mantle corner: ETS and silica deposition. J. Geophys. Res.: Solid Earth 120, 4344–4358.
Iriondo, A., 2001. Proterozoic Basements and Their Laramide Juxtaposition in NW Sonora Mexico–tectonic Constraints on the SW Margin of Laurentia. Ph.D. thesis, Boulder University of Colorado, p. 222.

Isozaki, Y., Aoki, K., Nakama, T., Yanai, S., 2010. New insight into a subduction-related orogen: a reappraisal of the geotectonic framework and evolution of the Japanese Island. Gondwana Res. 18, 82–105.
Jackson, J., Molnar, P., 1990. Active faulting and block rotations in the western Transverse Ranges, California. Tectonics 5, 629–648.
Johnson, S.P., Thorne, A.M., Tyler, A.M., Korch, R.J., Kennett, B.L.N., Cutten, H.N., Goodwin, J., Blay, O., Blewitt, R.S., Joly, A., Dentith, M.C., Aitkin, A.R.A., Holzschuh, J., Salmon, M., Reading, A., Heinson, G., Boreng, G., Ross, J., Costello, R.D., Fomin, T., 2006. Crustal architecture of the Capricorn orogen, western Australia, and associated metallogeny. Aust. J. Earth Sci. 60, 681–705.
Joly, A., McCuaig, T.C., Bagas, L., 2010. The importance of early crustal architecture for subsequent basin-forming, magmatic and fluid flow events. The Granites-Tanami Orogen example. Precambrian Res. 182, 15–29.
Katayama, I., Terada, T., Okazaki, K., Tanikawa, W., 2012. Episodic tremor and slow slip potentially linked to permeability contrasts at the Moho. Nat. Geosci. 5, 731–734.
Kawai, K., Tsuchiya, T., Tsuchiya, J., Maruyama, S., 2009. Lost primordial continents. Gondwana Res. 16, 581–586.
Kennedy, B.M., Kharaka, Y.K., Evans, W.C., Ellwood, A., DePaolo, D.J., Thordsen, J., Ambats, G., Mariner, R.H., 1997. Mantle fluids in the san Andreas Fault system, California. Science 278, 1278–1281.
Kennedy, B.M., van Soest, M.C., 2007. Flow of mantle fluid through the ductile lower crust: helium isotope trends. Science 318, 1433–1436.
Klein-BenDavid, O., Pettke, T., Kessel, R., 2011. Chromium mobility in hydrous fluids at upper mantle conditions. Lithos 125, 122–130.
Klemperer, S.L., Kennedy, B.M., Sastry, S.R., Makovsky, Y., Harinarayana, T., Leech, M., 2013. Mantle fluids in the Karakoram fault: helium isotope evidence. Earth Planet. Sci. Lett. 366, 59–70.
Knight, J.T., Groves, D.I., Ridley, J.R., 1993. The Coolgardie Goldfield, Western Australia: district-scale controls on an Archaean gold camp in an amphibolite facies terrane. Miner. Depos. 28, 436–456.
Knox-Robinson, C.M., Wyborn, L.A.I., 1997. Towards a holistic exploration strategy: using geographic information systems as a tool to enhance exploration. Aust. J. Earth Sci. 44, 453–463.
Kolb, J., Dziggel, A., Bagas, L., 2015. Hypozonal lode gold deposits: a genetic concept based on a review of the New Consort, Renco, Hutti, Hira Buddini, Navachab, Nevoria and The Granites deposits. Precambrian Res. 262, 20–44.
Kolb, J., Meyer, M.F., 2002. Fluid inclusion record of the hypozonal orogenic Renco gold deposit (Zimbabwe) during the retrograde P–T evolution. Contrib. Mineral. Petrol. 143, 495–509.
Kolb, J., Rogers, A., Meyer, F.M., 2005. Relative timing of deformation and two-stage gold mineralization at Hutti mine, Dharwar Craton, India. Miner. Depos. 40, 156–174.
Kolb, J., Sindern, S., Kisters, A.F.M., Meyer, F., Hoernes, S., Schneider, J., 2005. Timing of Uralian orogenic gold mineralization at Kochkar in the evolution of the East Uralian granite-gneiss terrane. Miner. Depos. 40, 473–491.
Kontak, D.J., Smith, P.K., Kerrich, R., Williams, P.F., 1990. Integrated model for Meguma group lode gold deposits, Nova Scotia, Canada. Geology 18, 238–242.
LaFlamme, C., Jamieson, J.W., Fiorentini, M.L., Thebaud, N., Caruso, S., Selvaraja, V., 2018. Investigating sulfur pathways through the lithosphere by tracing mass independent fractionation of sulfur to the Lady Bountiful orogenic gold deposit, Yilgarn Craton. Gondwana Res. 58, 27–38.
Large, R.R., Bull, S.W., Maslennikov, V.V., 2011. A Carbonaceous sedimentary source-rock model for Carlin-type and orogenic gold deposits. Econ. Geol. 106, 331–358.
Large, R.R., Danyushevsky, L.V., Hollit, C., Maslennikov, V., Meffre, S., Gilbert, S., Bull, S., Scott, R., Emsbo, P., Thomas, H., Foster, J., 2009. Gold and trace element zonation in pyrite using a laser imaging technique: implications for the timing of gold in orogenic and Carlin-style sediment- hosted deposits. Econ. Geol. 104, 635–668.
Large, R.R., Halpin, J.A., Danyushevsky, L.V., Maslennikov, V.V., Bull, S.W., Long, J.A., Gregory, D.D., Lounejeva, E., Lyons, T.W., Sack, P.J., McGoldrick, P.J., Calver, C.R., 2014. Trace element content of sedimentary pyrite as a new proxy for deep-time ocean-atmosphere evolution. Earth Planet. Sci. Lett. 389, 209–220.
Leader, L.D., Robinson, J.A., Wilson, C.J.L., 2010. Role of faults and folding in controlling gold mineralization at Fosterville, Victoria. Aust. J. Earth Sci. 57, 259–277.
Li, N., Chen, Y.J., Santosh, M., Pirajno, F., 2015. Compositional polarity of Triassic granitoids in the Qinling Orogen, China: implication for termination of the northernmost paleo-Tethys. Gondwana Res. 27, 244–257.
Li, N., Chen, Y.J., Santosh, M., Pirajno, F., 2015. Compositional polarity of Triassic granitoids in the Qinling Orogen, China: implications for termination of northernmost paleo-Tethys. Gondwana Res. 27, 244–257.
Li, N., Deng, J., Yang, L.Q., Groves, D.I., Liu, X., Dai, W.G., Li, N., 2018. Constraints on depositional conditions and ore-fluid source for orogenic gold districts in the West Qinling Orogen, China: implications from sulfide assemblages and their trace-element geochemistry. Ore Geol. Rev. 102, 204–209.
Li, S.R., Santosh, M., 2017. Geodynamics of heterogeneous gold mineralization in the North China Craton and its relationship to lithospheric destruction. Gondwana Res. 50, 267–292.
Li, L., Santosh, M., Li, S.-R., 2015. The Jiaodong-type gold deposits—characteristics, origin and prospecting. Ore Geol. Rev. 65, 589–611.
Loucks, R.R., Mavrogenes, J.A., 1999. Gold solubility in supercritical hydrothermal brines measured in synthetic fluid inclusions. Science 284, 2159–2163.
Mair, J., Farmer, L., Groves, D., Hart, C., Goldfarb, R., 2011. Petrogenesis of mid-Cretaceous post-collisional magmatism at Scheelite Dome, central Yukon Territory, Canada—evidence for a lithospheric mantle source. Econ. Geol. 106, 451–480.
Maruyama, S., Hasegawa, A., Santosh, M., Kogiso, T., Zhao, D., 2009. The dynamics of big mantle wedge, magma factory, and metamorphic-metasomatic factor in subduction zones. Gondwana Res. 16, 3–4.
Maruyama, S., Liou, J.G., Terabayashi, M., 1996. Blueschists and eclogites of the world and their exhumation. Int. Geol. Rev. 38, 485–594.
Matsuda, T., Isozaki, Y., 1991. Well-documented travel history of Mesozoic pelagic chert in Japan: from remote ocean to subduction zone. Tectonics 10, 475–499.
McCuaig, T.C., Beresford, S., Hronsky, J., 2010. Translating the mineral systems approach into an effective exploration targeting system. Ore Geol. Rev. 38, 128–138.
McCuaig, T.C., Kerrich, R., Groves, D.I., Archer, N., 1993. The nature and dimensions of regional and local gold-related hydrothermal alteration in tholeiitic metabasalts in the Norseman Goldfields–the missing link in a crustal continuum of gold deposits? Miner. Depos. 28, 420–435.
McNaughton, N.J., Groves, D.I., Witt, W.K., 1993. The source of lead in Archaean lode-gold deposits of the Menzies-Kalgoorlie-Kambalda region, Yilgarn Block, Western Australia. Miner. Depos. 28, 495–502.
McCuaig, T.C., Hronsky, J.M.A., 2014. The Mineral System Concept: the Key to Exploration Targeting. SEG 2014: Building Exploration Capability for the 21st Century, pp. 153–175.
Megill, R.E., 1988. Exploration Economics. PennWell, Tulsa, p. 238.
Miller, J.M., Adams, G., 2013. The amphibolite-facies lindsays deposit, coolgardie goldfield, Yilgarn craton, western Australia–a type example of the crustal continuum model? 12th biennial SGA meeting. Proceedings 3, 1156–1159. Uppsala, Sweden.
Moresi, L., Betts, P.G., Miller, M.S., Cayley, R.A., 2014. Dynamics of continental accretion. Nature 508, 245–248.
Mueller, A.G., Harris, L.B., Lungan, A., 1988. Structural control on greenstone-hosted gold mineralization by transcurrent shearing: a new interpretation of the Kalgoorlie mining district, Western Australia. Ore Geol. Rev. 3, 359–387.
Neumayr, P., Cabri, L.J., Groves, D.I., Mikucki, E.J., Jackman, J.A., 1993. The mineralogical distribution of gold and relative timing of gold mineralization in two Archean settings of high metamorphic grade in Australia. Can. Mineral. 31, 711–725.
Nicholson, C., Seeber, L., Williams, P., Sykes, L.R., 1986. Seismic evidence for conjugate slip and block rotation within the San Andreas Fault system, California. Tectonics 5, 629–648.
Ojala, V.J., Ridley, J.R., Groves, D.I., Hall, G.C., 1993. The Granny Smith gold deposit: the role of heterogeneous stress distribution at an irregular granitoid contact in a greenschist facies terrane. Miner. Depos. 28, 409–419.
Owen, A.J., Coleby, B.R., Drummond, B.J., 1991. Eastern Goldfields Deep Crust Seismic Reflection Survey, Yligarn Block, Western Australia: Stacked and Migrated Seismic Data and Images for Lines EGF-1, EGF-2, and EGF-3. Geoscience Australia Website.
Page, R.A., Plafker, G., Pulpan, H., 1995. Block rotations in east-central Alaska: a framework for evaluating earthquake potential? Geology 23, 629–632.
Peacock, S.M., Christensen, N.I., Bostock, M.G., Audet, P., 2011. High pore pressures and porosity at 35 km depth in the Cascadia subduction zone. Geology 39, 471–474.
Perring, C.S., Groves, D.I., Ho, S.E., 1987. Constraints on the source of auriferous fluids for Archaean gold deposits. In: Ho, S.E., Groves, D.I. (Eds.), Recent Advances in Understanding Precambrian Gold Deposits. Publication 11. Geology Department and University Extension, University of Western Australia, pp. 287–306.
Phillips, G.N., Groves, D.I., Martyn, J.E., 1984. An epigenetic origin for banded iron-formation- hosted gold deposits. Econ. Geol. 79, 162–171.
Phillips, G.N., Powell, R., 2010. Formation of gold deposits-a metamorphic devolatilization model. J. Metamorph. Geol. 28, 689–718.
Pili, E., Kennedy, B.M., Conrad, M.E., Gatier, J.-P., 2011. Isotopic evidence for the infiltration of mantle and metamorphic CO_2-H_2O fluids from below in faulted rocks from the San Andreas Fault system. Chem. Geol. 281, 242–252.
Pitcairn, I.K., Craw, D., Teagle, D.A.H., 2015. Metabasalts as sources of metals in orogenic gold deposits. Miner. Depos. 50, 373–390.
Pitcairn, I.K., Teagle, D.A.H., Craw, D., Olivo, G.R., Kerrich, R., Brewer, T.S., 2006. Sources of metals and fluids in orogenic gold deposits: insights from the Otago and Alpine Schists, New Zealand. Econ. Geol. 101, 1525–1546.
Radhakrishna, B.P., Curtis, L.C., 1999. Gold in India. Geological Society of India, Bangalore, p. 307.
Ridley, J.R., 1993. The relations between mean rock stress and fluid flow in the crust: with reference to vein- and lode-style gold deposits. Ore Geol. Rev. 8, 23–37.
Ridley, J.R., Diamond, L.W., 2000. Fluid chemistry of orogenic lode gold deposits and implications for genetic models. Rev. Econ. Geol. 13, 141–162.
Robert, F., Poulson, H.K., Cassidy, K.F., Hodgson, J.C., 2005. Gold metallogeny of the superior and Yilgarn cratons. In: Economic Geology 100th Anniversary, pp. 1001–1033.
Rock, N.M.S., Groves, D.I., Perring, C.S., Golding, S.D., 1989. Gold, lamprophyres, and porphyries: what does their association mean? Econ. Geol. Monogr. 6, 609–625.
Rospabé, M., Ceuleneer, G., Benoit, M., Abily, B., Pinet, P., 2017. Origin of the dunitic mantle-crust transition zone in the Oman ophiolite: the interplay between percolating magmas and high-temperature hydrous fluids. Geology 45, 471–474.
Ryan, R.J., Smith, P.K., 1998. A review of the mesothermal gold districts of the Meguma Group, Nova Scotia Canada. Ore Geol. Rev. 13, 153–183.
Safonova, I.Y., Utsunomia, A., Kojima, S., Nakae, S., Tomurfogoo, O., Filippov, A.N., Koizumi, K., 2009. Pacific superplume-related oceanic basalts hosted by accretionary complex of Central Asia, Russian Far East and Japan. Gondwana Res. 16, 587–608.
Santosh, M., 2010. A synopsis of recent conceptual models on supercontinent tectonics in relation to mantle dynamics, life evolution and surface environment. J. Geodyn. 50, 116–133.
Santosh, M., 2010. Assembling North China Craton within the Columbia supercontinent: the role of double-sided subduction. Precambrian Res. 178, 149–167.
Santosh, M., Maruyama, S., Omori, S., 2009. A Fluid Factory in Solid Earth, vol 1. Geological Society of America, Lithosphere, pp. 29–33.
Santosh, M., Maruyama, S., Sato, K., 2009. Anatomy of a Cambrian suture in Gondwana: pacific-type orogeny in southern India? Gondwana Res. 16, 321–341.

Sarma, D.S., Fletcher, I.R., Rasmussen, B., McNaughton, N.J., Mohan, M.R., Groves, D.I., 2011. Archaean gold mineralization synchronous with late cratonization of the Western Dharwar Craton, India: 2.52 Ga U-Pb ages of hydrothermal monazite and xenotime in gold deposits. Miner. Depos. 46, 273–288.
Saunders, J.E., Pearson, N.J., O'Reilly, S.Y., Griffin, W.L., 2018. Gold in the mantle: a global assessment of abundance and redistribution processes. Lithos 322, 376–391.
Schodde, R., 2017. Long term trends in global exploration-Are we finding enough metals?. In: 8th Fennoscandian Exploration and Mining Conference. Levi, Finland, pp. 1–66.
Schrauder, M., Navon, O., 1994. Hydrous and carbonatitic mantle fluids in fibrous diamonds from Jwaneng, Botswana. Geochem. Cosmochim. Acta 58, 761–771.
Selvaraja, V., Caruso, S., Fiorentini, M.L., LaFlamme, C., Bui, T.-H., 2017. Atmospheric sulfur in the orogenic gold deposits of the Archean Yilgarn Craton, Australia. Geology 45, 691–695.
Seno, T., Kirby, S.H., 2014. Formation of plate boundaries: the role of mantle devolatilization. Earth Sci. Rev. 129, 85–99.
Sibson, R.H., 1992. Implications of fault-valve behaviour for rupture nucleation and recurrence. Tectonophysics 211, 282–293.
Sibson, R.H., 2004. Controls on maximum fluid overpressure defining conditions for mesozonal mineralization. J. Struct. Geol. 26, 1127–1136.
Sibson, R.H., 2013. Stress switching in subduction forearcs: implications for overpressure containment and strength cycling on megathrusts. Tectonophysics 600, 142–152.
Song, M.-C., Li, S.-Z., Santosh, M., Zhao, S.-J., Yu, S., Yi, P.-H., Cui, S.-X., Lu, G.-X., Xu, J.-X., Song, Y.-X., Zhou, M.L., 2015. Types, characteristics and metallogenesis of gold deposits in the Jiaodong Peninsula, eastern North China craton. Ore Geol. Rev. 65, 612–625.
Standish, C.D., Dhuime, B., Chapman, R.J., Hawkesworth, C.J., Pike, A.W.G., 2014. The genesis of gold mineralization hosted by orogenic belts: a lead isotope investigation of Irish gold deposits. Chem. Geol. 378–379, 40–51.
Steadman, J.A., Large, R.R., Meffre, S., Bull, S.W., 2013. Age, origin, and significance of nodule sulfides in 2680 Ma Carbonaceous black shale of the Eastern Goldfields Superterrane, Yilgarn craton, Western Australia. Precambrian Res. 230, 227–247.
Stern, R.C., 2011. Subduction erosion: rates, mechanisms, and its role in arc magmatism and the evolution of continental crust and mantle. Gondwana Res. 20, 284–308.
Straub, S.M., Zhellmer, G.F., 2012. Volcanic arcs as archives of plate tectonic change. Gondwana Res. 21, 495–516.
Tomkins, A.G., 2010. Windows of metamorphic sulfur liberation in the crust: implications for gold deposit genesis. Geochem. Cosmochim. Acta 74, 3246–3259.
Tripp, G., 2014. How Neoarchean stratigraphy and structural geology determine the timing and controls of world-class greenstone gold camps in the Eastern Goldfields Province: key factors for gold exploration. Gold'14 Extended Abstracts. Austr. Inst. Geosci. Bull. 59, 124–128.
Vannucchi, P., Morgan, J.P., Balestreiri, M.L., 2016. Subduction erosion, and the de-construction of continental crust: the Central America case and its global implications. Gondwana Res. 40, 184–198.
Vearncombe, J., Phillips, G.N., 2019. The importance of brownfields gold exploration. Miner. Depos. https://doi.org/10.1007/s00126-019-00897-1.
Vielreicher, N.M., Groves, D.I., McNaughton, N.J., 2016. The giant Kalgoorlie Goldfield revisited. Geosci. Front. 7, 359–374.
Vielreicher, N.M., Groves, D.I., Snee, L.W., Fletcher, I.R., McNaughton, N.J., 2010. Broad synchroneity of three gold mineralization styles in the Kalgoorlie gold field– SHRIMP, U-Pb, and $^{40}Ar/^{39}Ar$ geochronological evidence. Econ. Geol. 105, 187–227.
Wang, Q.F., Groves, D.I., Deng, J., Li, H., Yang, L., Dong, C., 2019. Evolution of the Miocene Ailaoshan gold deposits, southeastern Tibet, during a complex tectonic history of lithosphere-crust interaction. Miner. Depos. https://doi.org/10.1007/s00126-019-00922-3.
Wang, L.G., Qiu, Y.M., McNaughton, N.J., Groves, D.I., Luo, Z.K., Huang, J.Z., Miao, L.-C., Liu, Y.K., 1998. Constraints on crustal evolution and gold metallogeny in the northwestern Jiaodong Peninsula, China, from SHRIMP U–Pb zircon studies of granitoids. Ore Geol. Rev. 13, 275–291.
Wang, R., Cudahy, T., Laukamp, C., Walshe, J.L., 2017. White mica as a hyperspectral tool in exploration for the Sunrise Dam and Kanowna Belle gold deposits, Western Australia. Econ. Geol. 112, 1153–1176.
Wang, Q.F., Zhao, H.S., Groves, D.I., Deng, J., Zhang, Q., Xue, S., 2019. Role of metasomatized mantle lithosphere in the genesis of the Jurassic Danba hypozonal orogenic gold deposit, western China. Miner. Depos. https://doi.org/10-1007/s00126-015-00928-x.
Webber, A.P., Roberts, S., Taylor, R.N., Pitcairn, I.K., 2013. Golden plumes—substantial gold enrichment of oceanic crust during ridge-plume interaction. Geology 41, 87–90.
Weinberg, R.F., Hodkiewitcz, P.F., Groves, D.I., 2004. What controls gold distribution in Archean terranes? Geology 32, 545–548.
Weinberg, R.F., van der Borgh, P., Bateman, R.J., Groves, D.I., 2006. Kinematic history of the boulder-lefroy shear zone system and controls on associated gold mineralization, Yilgarn craton, western Australia. Econ. Geol. 100, 1407–1426.
White, A.J.R., Waters, D.J., Robb, L.J., 2015. Exhumation-driven devolatilization as a fluid source for orogenic gold mineralization at the Damang deposit, Ghana. Econ. Geol. 110, 1009–1026.
Wilson, C.J.L., Schaubs, P.M., Leader, L.D., 2013. Mineral precipitation in the quartz reefs of the Bendigo gold deposit, Victoria, Australia. Econ. Geol. 108, 259–278.
Windley, B.F., Maruyama, S., Xiao, W.-J., 2010. Delamination/thinning of subcontinental lithospheric mantle under eastern China–the role of water and multiple subduction. Am. J. Sci. 310, 1250–1293.
Witt, W.K., Ford, A., Hanrahan, B., Mamuse, A., 2013. Regional-scale targeting for gold in the Yilgarn craton: Part 1 of the Yilgarn gold exploration targeting atlas. Geol. Surv. West. Austr. Rep. 125, 130.
Wyborn, L.A.I., Heinrich, C.A., Jaques, A.L., 1994. Australian Proterozoic Mineral Systems: Essential Ingredients and Mappable Criteria. Australasian Institute of Mining and Metallurgy Annual Conference, Melbourne, pp. 109–115.
Wyman, D., Kerrich, R., 2010. Mantle plume-volcanic arc interaction—consequences for magmatism, metallogeny, and cratonization in the Abitibi and Wawa subprovinces, Canada. Can. J. Earth Sci. 47, 565–589.
Wyman, D.A., Cassidy, K.F., Hollings, P., 2016. Orogenic gold and the mineral systems approach: resolving fact, fiction and fantasy. Ore Geol. Rev. 78, 322–335.
Wyman, D.A., Kerrich, R., 2002. Formation of Archean continental lithospheric roots: the role of mantle plumes. Geology 30, 543–546.
Wyman, D.A., O'Neill, C.O., Ayer, J.A., 2008. Evidence for Modern-Style Subduction to 3.1Ga: a Plateau-Adakite-Gold (Diamond) Association, vol 440. Geological Society of America Special Publication, pp. 129–148.
Xiao, W.J., Sun, M., Santosh, M., 2015. Continental reconstruction and metallogeny of the Circum-Junggar areas and termination of the southern Central Asian Orogenic Belt. Geosci. Front. 6, 137–140.
Yamamoto, S., Senshu, H., Omori, S., Maruyama, S., 2009. Granite subduction, arc subduction, tectonic erosion and sediment subduction. Gondwana Res. 15, 443–453.
Yang, L.Q., Deng, J., Guo, R.P., Guo, L.N., Wang, Z.L., Chen, B.H., Wang, X.D., 2015. World-class Xincheng gold deposit: an example from the giant Jiaodong gold province. Geosci. Front. 7, 419–430.
Yang, L.Q., Deng, J., Guo, L.N., Wang, Z.L., Li, X.Z., Li, J.L., 2016. Origin and evolution of ore fluid, and gold-deposition processes at the giant Taishang gold deposit, Jiaodong peninsula, eastern China. Ore Geol. Rev. 72, 585–602.
Yang, L.Q., Deng, J., Wang, Z.L., Guo, L.N., Li, R.H., Groves, D.I., Danyushevkiy, L.V., Zhang, C., Zheng, X.L., Zhao, H., 2016. Relationships between gold and pyrite at the Xincheng gold deposit, Jiaodong Peninsular, China: implications for gold source and deposition in a brittle epizonal environment. Econ. Geol. 111, 105–126.
Yang, Q.Y., Santosh, M., 2015. Early Cretaceous magma flare-up and its implications on gold mineralization in the Jiaodong Peninsula, China. Ore Geol. Rev. 65, 626–642.
Yang, C.X., Santosh, M., 2020. Ancient deep roots for Mesozoic world-classs gold deposits in the north China craton: an integrated genetic perspective. Geosci. Front. 11, 203–214.
Yang, Q.Y., Santosh, M., Shen, J.F., Li, S.R., 2014. Juvenile vs. recycled crust in NE China: zircon U–Pb geochronology, Hf isotope and an integrated model for Mesozoic gold mineralization in the Jiaodong Peninsula. Gondwana Res. 25, 1445–1468.
Zhang, L., Groves, D.I., Yang, L.Q., Sun, S.C., Weinberg, R.F., Wang, J.X., Wu, S.G., Gao, L., Yuan, L.L., Li, R.H., 2019a. Utilization of pre-existing competent and barren quartz veins as hosts to later orogenic gold ores at the Huangjindong gold deposit, Jiangnan Orogen, southern China. Miner. Depos. https://doi.org/10.1007/s00126-019-00904-5.
Zhang, L., Groves, D.I., Yang, L.Q., Wang, G.W., Liu, X.D., Li, D.P., Song, Y.X., Shan, W., Sun, S.C., Wang, Z.-K., 2019b. Relative roles of formation and preservation on gold endowment along the Sanshandao Gold Belt, Jiaodong Province, China: importance for province-to district-scale gold exploration. Miner. Depos. https://doi.org/10.1007/s00126-019-00908-1.
Zhang, L., Weinberg, R.F., Yang, L.Q., Groves, D.I., Sai, S.X., Matchan, E., Phillips, D., Kohn, B.P., Miggins, D.P., Liu, Y., Deng, J., 2020. Mesozoic orogenic gold mineralization in the Jiaodong Peninsula, China: a focused event at ca. 120 Ma during cooling of pre-gold granite intrusions. Economic Geology, 115, 415-441. https://doi.org/10.5382/econgeo.4716.
Zhang, L., Yang, L.Q., Groves, D.I., Liu, Y., Sun, S.C., Qi, P., Wu, S.G., Peng, J.S., 2018. Geological and H–O–S–Pb isotopic constraints on ore genesis, Huangjindong goldfield, Jiangnan Orogen, southern China. Ore Geol. Rev. 99, 264–281.
Zhao, H.S., Wang, Q.F., Groves, D.I., Deng, J., 2019. A rare Phanerozoic amphibolite-hosted gold deposit at Danba, Yangtze Craton, China: significance to fluid and metal sources for orogenic gold systems. Miner. Depos. 54, 133–152.
Zhao, J.H., Zhou, M.F., 2008. Neoproterozoic adakitic plutons in the northern margin of the Yangtze block, China: partial melting of a thickened lower crust and implications for secular crustal evolution. Lithos 104, 231–248.
Zhou, M.F., Yan, D.P., Kennedy, A.K., Li, Y.Q., Ding, J., 2002. SHRIMP zircon geochronological and geochemical evidence for Neoproterozoic arc-related magmatism along the western margin of the Yangtze Block, South China. Earth Planet. Sci. Lett. 196, 51–67.

David Groves is Emeritus Professor in the Centre for Exploration Targeting at the University of Western Australia (UWA) and Visiting Professor at the China University of Geosciences Beijing. Educated at Varndean Grammar School in Brighton, UK, and Hobart High School, Tasmania. BSc Honours (First Class) and PhD from the University of Tasmania, Honorary DSc from UWA. Former Director of Key Centre for Strategic Mineral Deposits and Centre for Global Metallogeny at UWA. Supervised over 250 BSc Honours, MSc and PhD students. Published approximately 500 papers and book chapters. Former President of Geological Society of Australia, SEG and SGA. Awarded 11 Research Medals including Gold Medals of SEG and SGA and the Geological Association of Canada Medal, plus other medals from Australia, South Africa and UK. Currently Consultant to the mineral exploration industry and brokers and investors in Canada with exploration properties in Africa, South America and Greenland. Most recently a novelist The Digital Apocalypse, The Plagues' Protocol and Destiny on Magic White Mountain.

M. Santosh is Professor at the China University of Geosciences Beijing (China), Specially Appointed Foreign Expert of China, Professor at the University of Adelaide, Australia and Emeritus Professor at the Faculty of Science, Kochi University, Japan. PhD (Cochin University of Science and Technology, India), D.Sc. (Osaka City University, Japan) and D.Sc. (University of Pretoria, South Africa). He is the Founding Editor of Gondwana Research as well as the founding Secretary General of the International Association for Gondwana Research. Research fields include petrology, fluid inclusions, geochemistry, geochronology, metallogeny and supercontinent tectonics. Published over 800 research papers, edited several memoir volumes and journal special issues, and co-author of the book 'Continents and Supercontinents' (Oxford University Press, 2004). Recipient of National Mineral Award, Outstanding Geologist Award, Thomson Reuters 2012 Research Front Award, Thomson Reuters High Cited Researcher 2014, 2015, 2016, 2017, 2018 and 2019.

Liang Zhang is a Post-doctoral Fellow at China University of Geosciences, Beijing (CUGB). He obtained a B.Eng. (2011) from Hebei GEO University, was a Visiting Ph.D. student (2015) at Monash University, and received his Ph.D. from CUGB (2016). He has published more than 20 research papers as either first or co-author. He has been the recipient of Scientific and Technological Progress Awards (First prize, Ministry of Education, China, 2014; Second prize, Shandong Province, China, 2014; First prize, China Gold Association, 2012 and 2013).